Nano Research Energy

ISSN 2791-0091 (print); 2790-8119 (online)
https://doi.org/10.26599/NRE.2022.9120029

Review Article

Te-mediated electro-driven oxygen evolution reaction

Feng Gao[1], Jiaqing He[1], Haowei Wang[1], Jiahui Lin[1], Ruixin Chen[1], Kai Yi[1], Feng Huang[1], Zhang Lin[2,3], Mengye Wang[1] (✉)

[1] State Key Laboratory of Optoelectronic Materials and Technologies, School of Materials, Sun Yat-sen University, Guangzhou 510275, China
[2] School of Environment and Energy, Key Laboratory of Pollution Control and Ecosystem Restoration in Industry Clusters (Ministry of Education), South China University of Technology, Guangzhou 51006, China
[3] School of Metallurgy and Environment, Central South University, Changsha 410083, China

Received: 4 July 2022 / **Revised:** 13 August 2022 / **Accepted:** 15 August 2022

ABSTRACT

In the 21st century, the rapid development of human society has made people's demand for green energy more and more urgent. The high-energy-density hydrogen energy obtained by fully splitting water is not only environmentally friendly, but also is expected to solve the problems caused by the intermittent nature of new energy. However, the slow kinetics and large overpotential of the oxygen evolution reaction (OER) limit its application. The introduction of Te element is expected to bring new breakthroughs. With the least electronegativity among the chalcogens, the Te element has many special properties, such as multivalent states, strong covalentity, and high electrical conductivity, which make it a promising candidate in electrocatalytic OER. In this review, we introduce the peculiarities of Te element, summarize Te doping and the extraordinary performance of its compounds in OER, with emphasis on the scientific mechanism behind Te element promoting the OER kinetic process. Finally, challenges and development prospects of the applications of Te element in OER are presented.

KEYWORDS

oxygen evolution reaction, telluride, electrocatalyst, water splitting, chalcogen

1 Introduction

From the perspective of historical development, every energy innovation of human beings is a huge progress in human technology and social development [1]. Nowadays, human beings mainly rely on fossil energy, but the problems of non-renewable fossil energy and the destruction of the ecological environment caused by the exploitation and use of fossil energy have become more and more serious [2]. Humans have begun to face severe challenges such as energy depletion and climate deterioration, but human demand for energy is increasing day by day. So we have to find new green energy to replace traditional fossil energy, such as wind energy, water energy, and solar energy [3, 4]. It is a pity that these new energy sources are all intermittent energy sources. But if they are directly integrated into the grid, they will have an impact on the grid [5, 6]. So, we need a technology that captures this intermittent energy and stores it, such as liquid fuels and batteries [7–10]. One of the most attractive solutions is to convert these intermittent green energy into hydrogen energy to store first, and then use fuel cell technology to generate electricity when we need it [11, 12]. And a more attractive way of this kind of energy conversion is total water splitting, which is completely green and environmentally friendly, with abundant raw materials, and is expected to be practical [13].

The total water splitting is divided into two half-reactions, the cathodic hydrogen evolution reaction (HER) and the anodic oxygen evolution reaction (OER) [14]. Among them, OER involves the process of four-electron transfer, which is a complex proton-coupled electron transfer reaction and is kinetically limited and requires a large overpotential to proceed. This greatly limits the application of total water splitting [15]. OER has been extensively studied in both alkaline and acidic electrolyzers. In general, the recognized OER mechanism is the adsorbate evolution mechanism (AEM) [16]. There are four possible reaction steps under basic conditions as follows:

$$* + OH^- \rightleftharpoons *OH + e^- \quad (1)$$

$$*OH + OH^- \rightleftharpoons *O + H_2O + e^- \quad (2)$$

$$*O + OH^- \rightleftharpoons *OOH + e^- \quad (3)$$

$$*OOH + OH^- \rightleftharpoons H_2O + O_2 + e^- \quad (4)$$

The reaction steps under acidic conditions are as follows:

$$* + H_2O \rightleftharpoons *OH + e^- + H^+ \quad (5)$$

$$*OH \rightleftharpoons *O + e^- + H^+ \quad (6)$$

$$*O + H_2O \rightleftharpoons *OOH + e^- + H^+ \quad (7)$$

Address correspondence to wangmengye@mail.sysu.edu.cn

$$*OOH \rightleftharpoons * + O_2 + e^- + H^+ \quad (8)$$

Among them, * represents the active site of the catalyst. It can be seen from the above reaction formulas that OER is essentially a heterogeneous reaction of four-electron and -proton coupling, which is related to three oxygen intermediates *OH, *O, and *OOH at the interface between the catalyst and water. If a reversible hydrogen electrode is used as the reference electrode, the thermodynamic potential of the OER is 1.23 V (vs. reversible hydrogen electrode (RHE)), independent of the electrolyte. In fact, the details of the OER reaction are still very complex, and a huge kinetic barrier needs to be overcome, which leads to the fact that the applied potential for the actual reaction is usually much higher than the standard thermodynamic potential [17]. Therefore, a great deal of work by countless scientific researchers has been devoted to developing an efficient and stable OER catalyst. At present, many high-efficiency catalysts have been developed, such as RuO_2, IrO_2, transition metal oxides, sulfides, selenides, phosphides, and borides, and the overpotential is greatly reduced to less than 200 mV [18–23]. Recently, Te metal and its compounds have exhibited extraordinary OER activity, becoming a very promising class of OER catalysts.

Te is the 52nd element in the periodic table, belonging to the VI A group, and is a member of the chalcogen. Its valence electron shell is $4d^{10}5s^2p^4$, so it has abundant valence states (such as ±2, +4, +6), which also endow it with special electronic properties. Since Te is in the fifth period, compared with the O, S, and Se in the same group, it has a larger atomic radius (1.43 Å) and anion radius (Te^{2-}, 2.21 Å). Electronegativity, which describes the ability of an atom to withdraw electrons, is another very important parameter. Te possesses a smaller electronegativity (2.10), so its ability to capture electrons is relatively weak.

The above characteristics determine that Te is a very special metalloid element. Te has abundant valence states, so it can play both anion and cation roles in catalysts, with a variety of effects in the catalytic process. And the high valence state of Te^{6+} in Te is likely to have a promoting effect in OER. The arrangement of the valence electron shell of Te implies that it has a special structure and novel electronic properties. For example, the crystal of the element Te is composed of special helical chains, which are often widely studied as p-type thermoelectric materials. Recent studies have shown that tellurium crystals are also Weyl semiconductors with special topological properties [24]. These topological properties hold promise for high mobility, highly stable surfaces, and simultaneous charge and spin transport with spin selectivity. Taking advantage of these topological properties is expected to produce highly active and stable catalysts. Two-dimensional (2D) films and one-dimensional (1D) nanowires (NWs) made of Te also exhibit topological properties, and can effectively tune their electronic structure and carrier mobility by compressive strain [25]. Among them, 2D tellurenes have recently attracted much attention due to their unique helical chain structure and unique physical properties. It not only has the characteristics of large specific surface area, no dangling bonds and extraordinary stability in the air, but also has theoretical ultra-high carrier mobility (i.e., ~ 10^4–10^6 $cm^2 \cdot V^{-1} \cdot s^{-1}$) and large in-plane piezoelectric coefficient [26]. These properties make them very suitable for the catalysis [27].

Due to its low electronegativity and weak electron-attracting ability, Te tends to exhibit stronger metallicity and higher electrical conductivity (~ 1,000 $S \cdot m^{-1}$). Among oxides and chalcogenides, tellurides generally exhibit a smaller band gap, which is beneficial to improving the conductivity of the catalysts for highly active catalytic OER [28]. Moreover, the small electronegativity also makes the bonding of Te with other metal elements more covalent, and the strong covalentity in such metal-anion bonding can often improve the catalytic efficiency of OER. From a chemical point of view, the stronger the covalent bond between the metal and the anion, the more favorable the redox reaction of the metal center. Simultaneously, this can adjust the redox energy levels of the conduction band and valence band edge to align with water as much as possible, which is beneficial to splitting water [29]. The strong covalent nature of Te bonding also predicts its great potential in OER reactions.

Tuning the intrinsic activity of the catalyst's active sites and increasing the catalyst's electric conductivity are expected to further improve the catalytic performance, one of which is a feasible and very effective solution to add other cations to the catalyst. Through advanced characterization methods such as *in situ* Raman and synchrotron radiation, together with density functional theory (DFT) calculations, researchers have proposed that the active sites of these efficient catalysts are several cations, including Ru, Ir, Fe, Co, and Ni [30–34]. Among these, the most famous materials are NiFe-LDH (LDH = layered double hydroxide) [35–38] (in which Ni and Fe synergize), CoCu-LDH [39–41] (in which Co and Cu synergize), and high-entropy nanomaterials (those have recently attracted extensive attention) [42–44]. Theoretically, Te element can exist in the catalyst in the form of Te^{2+}, Te^{4+}, and Te^{6+}, which can act synergistically with other cations to accelerate the OER process and enhance the intrinsic activity of the catalyst.

Regulation of electrocatalytic efficiency by anions is considered to be another promising approach [45]. The anion radius is usually larger than the cation radius, so it plays an important role in the integrity of the crystal lattice, and the substitution of anions exhibits a huge impact on the properties of the crystal catalyst. It is generally believed that the influence of anions on the catalyst may have the following aspects: (1) They adjust the electronic structure of the crystal, such as reducing the band gap, increasing the carrier concentration, and enhancing the conductivity, thereby improving the performance of the catalyst [46]. (2) They form defects, or even destroy the crystal lattice and form amorphous structure. This can not only change the electronic structure, but also increase the surface area and expose more active sites [47, 48]. (3) They change the chemical environment and electronic structure of the active site, and adjust the adsorption energy of intermediate species, so as to achieve a smaller overpotential [49]. In recent years, sulfides, selenides, phosphides, borides, etc. have all shown excellent catalytic activity, even surpassing oxides and hydroxides which are traditionally considered as the ideal catalysts. Te can also be added to the catalyst as an anion Te^{2-}. Due to the large radius of Te^{2-}, the influence on the lattice will be intensive, which is conducive to the formation of a large number of defects and the increase of the number of active sites. Furthermore, Te^{2-} tends to form strong covalent bonds with metal sites, which can adjust the electronic structure and enhance the conductivity.

To sum up, the characteristics of Te element determine its special status in OER. As a special kind of semi-metal element, it will surely shine in OER. In view of the particularity of Te

element and its outstanding properties in OER, it is necessary to review its recent progress. We summarize the latest research on the applications of Te element in OER from the three parts, including Te doping to enhance OER catalyst activity, OER of noble metal telluride and OER of transition metal telluride. The improved efficiency of Te element doping and the mechanism of improving OER efficiency are summarized. Finally the issues and challenges on the development of Te-contained electrocatalysts are discussed.

2 Te in oxygen evolution reaction electrocatalyst

2.1 Tellurium doped catalysts

To enhance the efficiency of catalysts, doping is a common and very effective method [50–54]. Researchers prefer to dope good catalysts with Te element to obtain higher OER activity. Due to the special electronic structure and small electronegativity of Te, Te doping can optimize the conductivity and electronic structure of the catalyst, and its large ionic radius also enables it to distort the lattice and create defects. Current examples of improving the activity of OER catalysts through Te doping will be described and summarized below, such as Te-doped 2D black phosphorus (BP), metal-organic framework (MOF) catalysts, transition metal base-like LDHs, and some highly efficient oxides, hydroxides and sulfur genera.

Regarded as a potential high-performance electrocatalyst, 2D BP materials have received wide interest due to their fascinating properties [55], which has small band gap [56, 57], excellent room temperature hole mobility [58, 59] and large specific surface area [60]. In 2016, Yang, Bingchao et al. [61] introduced Te element into BP crystal. They successfully doped BP with a low concentration of Te (0.1% atomic ratio) through a high-voltage technique, and found that it promoted the hole mobility at room temperature (> 1,850 $cm^2 \cdot V^{-1} \cdot s^{-1}$) and enhanced the environmental stability. However, this high-voltage scheme is difficult to accomplish a high-concentration doping. Zhang, Z. M et al. [62] synthesized high-concentration doped and high-quality Te-doped BP single crystals by a chemical vapor transport (CVT) method in 2018 (Fig. 1(a)). After Te-doped BP nanosheets were obtained by a liquid phase exfoliation, they were deposited on a glassy carbon electrode to test the electrocatalytic performance. Compared with the undoped BP counterparts, Te-doped BP nanosheets exhibited obviously improved OER efficiency (Fig. 1(b)). The possible reason is that the radius and electronegativity of Te atoms are quite different from those of P atoms. The introduction of Te atoms into the lattice composed of P anions of BP crystals showed a huge impact on the lattice and changed the charge distribution and electronic properties of the crystals, thereby affecting the interaction of BP nanosheets with oxygen intermediates. In order to further explore the mechanism behind the dramatic performance improvement and reveal the specific active sites and microstructure of the catalyst at the atomic scale, Zhu, J. F. et al. [63] performed DFT calculations on Te-doped BP. First-principles calculations showed that Te atoms preferred to bond with each other and form a cluster in BP, and they could be further stabilized by various intrinsic defects (Stone-Wales, single-vacancy defects, and zigzag nanoribbons). The synergistic effect of the clusters formed by

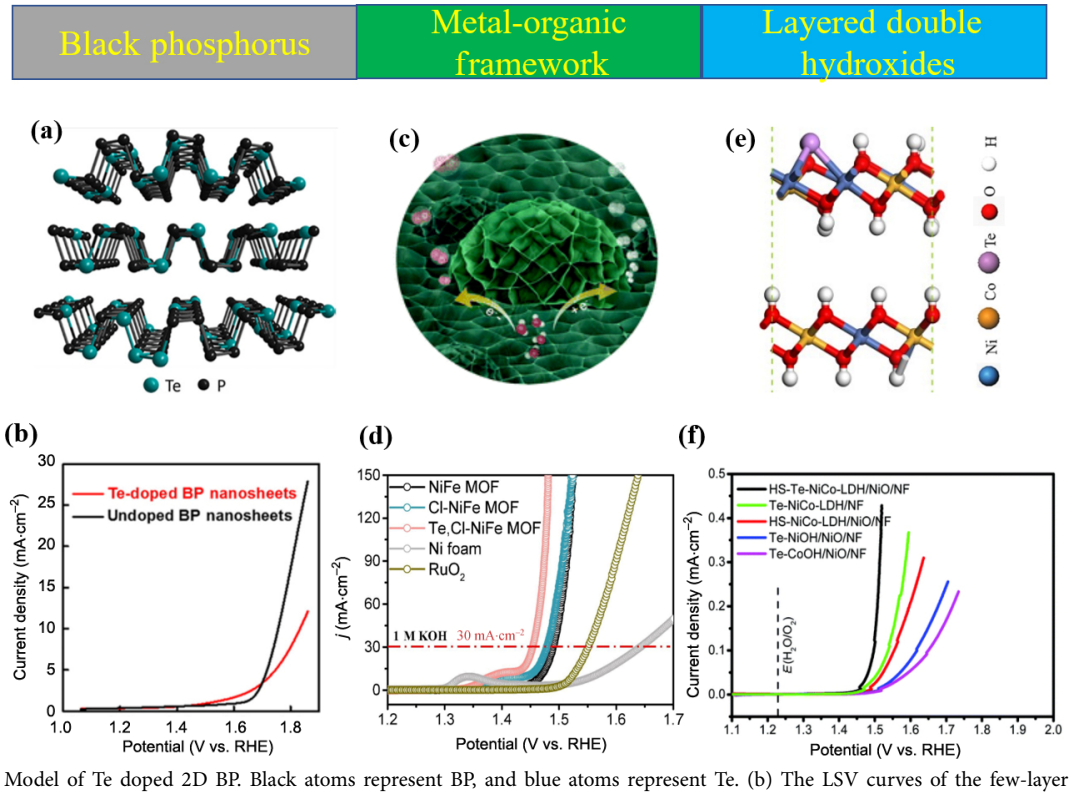

Figure 1 (a) Model of Te doped 2D BP. Black atoms represent BP, and blue atoms represent Te. (b) The LSV curves of the few-layer undoped and Te-doped BP nanosheets in 1 M KOH. (c) Model of MOF. It has a high specific surface area, which is beneficial to OER. (d) The LSV curves of the Te, Cl co-doped in 1 M KOH. (e) Model of Te doped NiCo-LDH. Purple atoms represent Te. (f) The LSV curves of the Te doped NiCo-LDH in 1 M KOH. Panels (a) and (b): reproduced with permission from Ref. [62], © American Chemical Society 2018. Panel (c): reproduced with permission from Ref. [64], © the Partner Organisations 2021. Panel (d): reproduced with permission from Ref. [65], © Elsevier B. V. 2022. Panels (e) and (f): reproduced with permission from Ref. [79], © Zhang, D. et al. 2022.

Te dopants and the inherent defects in BP reduced the binding strength of *O and optimized the adsorption energy of the intermediate species, thereby enhancing the catalytic activity of BP.

MOFs are another class of promising materials for water electrocatalysis, which possess a large number of active sites but low electrical conductivity (Fig. 1(c)) [64]. In order to improve its electric conductivity to further enhance the catalytic activity, doping Te becomes a good choice. In 2022, Keemin Park et al. [65] used chemical vapor deposition (CVD) to dope MOFs with Te, and achieved growing 2D nanosheets composing of Te and Cl co-doped NiFe MOFs on nickel foam. It showed a highly efficient OER in alkaline electrolyte with an overpotential of only 224 mV at 30 mA·cm^{-2} (Fig. 1(d)) and a stability of over 120 h. X-ray photoelectron spectroscopy (XPS) measurements demonstrated that Te behaved as a +4-valent cation in the catalyst, which significantly increased the oxidation state of Fe at the active site. This, thereby, adjusted the adsorption energy, improved the charge transfer process, and accelerated OER. In addition, MOF materials are often used to prepare porous carbon derivatives because of their porosity, large specific surface area, metal centers, and organic ligand binding. In 2022, Chengsi Hu et al. [66] successfully synthesized Te-doped ZnCo-MOF-derived porous carbon nanotubes (ZnCo-Te@NCs) by an *in-situ* formation and sacrificial template method on Te nanotube templates. Through XPS results, they found that Te exhibited both Te^{4+} and Te^{2-}. In O_2-saturated 0.1 M KOH solution, the overpotential was 400 mV at 10 mA·cm^{-2}, which was better than that of IrO_2 (426 mV). Meanwhile, the catalysts also exhibited excellent bifunctional electrocatalytic properties for application in zinc-air batteries with a large peak current density of 259.7 mW·cm^{-2} and excellent cycling durability.

Transition metal-based LDHs are also efficient OER catalysts, to which researchers have paid great attention [67, 68]. However, the application of these LDH materials as high-performance electrocatalysts is restricted by slow electron transport kinetics and instability due to their intrinsic low conductivity [69]. Metalloid-Te doping is expected to solve this problem. Metalloids can accept electrons from transition metals and then transfer electrons to adjacent oxygen atoms, which can lead to localized regions of electron enrichment or electron depletion on the surface of LDHs, thereby achieving the purpose of tuning the active site [70, 71]. Moreover, the electronic coupling interaction between the metalloid sp orbital and the metal d orbital can adjust the d orbital center and increase the density of electronic states near the Fermi level, thereby improving the conductivity of LDH [72]. In 2021, Lee, J. I. et al. [73] used a simple solvothermal method to grow Te-doped NiCo LDHs on 3D porous nickel foam (Fig. 1(e)). The doped Te preferentially entered the edge sites of transition metals (the true active sites in LDHs) and underwent strong covalent p–d hybridization with transition metals to form highly polarized local electronic structures. This enhanced the capability to accept the electron of OH^- and thus significantly enhanced the electrocatalytic OER activity. Among them, when the stoichiometric ratio of Te to Co was 0.6, the catalyst exhibited the best OER activity with extremely low overpotentials of 290 and 330 mV at 10 and 100 mA·cm^{-2}, respectively, and the Tafel slope was 45.48 mV·dec^{-1}. Electrochemical impedance spectroscopy (EIS) manifested that Te-doped NiCo LDHs (the stoichiometric ratio of Te to Co is 0.6) had a small charge transfer resistance (R_{ct} ~ 8 Ω), which implied that Te incorporation played an important role in facilitating the transfer of charges between the catalyst surface and the adsorbed reactants. In the same year, they also grew Te-doped $Ni(OH)_2$ crystallites on nickel foam by a hydrothermal method, which reached 10 and 100 mA·cm^{-2} at overpotentials of only 270 and 285 mV , and a very small Tafel slope of 26.9 mV·dec^{-1} in alkaline medium [74]. As metalloids can form strong covalent bonds with transition metals and can have various coordination forms, they can also play a role in stabilizing catalysts [75]. There are usually two phases of LDHs, namely α-phase and β-phase. α-phase LDHs display high activity but poor stability, which is very easy to transform into low-activity β-phase under alkaline conditions [76–78]. In 2022, Zhang, D. et al. [79] tried to use Te to improve the stability of the catalyst, and prepared honeycomb Te-doped NiCo LDHs through controllable anodic electrodeposition (ED) by a dynamic oxygen bubble template approach, which achieved an ultra-low overpotential of 221 mV at 10 mA·cm^{-2} (Fig. 1(f)). The doped Te existed in the form of Te^{4+} and had almost no effect on the valence states of other elements, which indicated that Te had no activity in the electrochemical reaction process. The X-ray diffraction (XRD) characterizations of the catalysts before and after the catalytic reaction indicated that honeycomb Te-doped NiCo LDHs still maintained the α phase with high catalytic activity after the electrochemical process under alkaline conditions, displaying unexpectedly excellent stability.

Besides, Te doping can improve the activity of some common oxides, hydroxides, chalcogenides, etc. In 2019, Wang, Y. et al. [80] prepared sandwich-like Te-doped $CoTe_{2x}Se_{2(1-x)}$ catalysts. By optimizing the amount of Te doping, the as-obtained catalysts possessed better OER performance than those of undoped binary pure $CoSe_2$ and $CoTe_2$ species. After composition optimization, the sandwich-like $Co(Te_{0.33}Se_{0.67})_2$ exhibited a better OER performance than the most advanced transition metal dichalcogenide (TMD) catalysts recently published in top journals. It has an onset potential of about 1.48 V, an overpotential of about 272 mV, and a Tafel slope of only 44 mV·dec^{-1}. After 3,000 cycles, the overpotential just exhibited a negligible increase. The stability was further investigated by chronopotentiometry, and its long-term stability remained over 50 h, with only a slight overpotential change of about 12 mV after 50 h. The authors believed that the slight structure distortion and abundant defects produced by Te anion doping were beneficial to exposing more active edge sites and enhancing the conductivity of the catalyst, which greatly improved the OER activity of the catalyst. Ibraheem, S. et al. [81] fabricated Te-doped FeNiOOH nanocubes through a controllable hydrothermal process. The catalysts simultaneously exhibited good OER and HER performance with low overpotentials of 167 and 22 mV, respectively, at 10 mA·cm^{-2}. Transmission electron microscopy (TEM) manifested that Te doping still retained its unique nanocubic structure, ensuring the exposure of its active sites. Te doping can also activate the edge-enriched Fe sites and enhance the adsorption capacity of the catalyst to oxidize intermediates during the OER/HER process, thereby improving the electrocatalytic performance. Wu, X. J. et al. [82] crafted Te-doped iron-based catalysts with crystalline and amorphous nanosheet structures on iron foams by CVD and ED methods, in which amorphous catalysts exhibited more pronounced electrocatalytic OER performance in alkaline electrolyte, requiring only an overpotential of 264.4 mV to reach a current density of 10 mA·cm^{-2} and a Tafel slope of

54.2 mV·dec^{-1}. The reason for the high activity is that the unique nanosheet morphology of the catalyst exposed more catalytically active sites, guaranteed the faster electron transfer and higher catalytic kinetics caused by Te doping. Li, G. R. et al. [83] prepared Te-doped Co_3O_4 nanomaterials by a simple hydrothermal method, obtaining an overpotential as low as 313 mV and a Tafel slope of 75 mV·dec^{-1}, which is superior to pure Co_3O_4 materials. XPS showed that Te existed in the form of Te^{2-}. TEM showed that the large-radius Te ions distorted the lattice and limited the growth of the crystal, thereby exposing more active sites. Raman analysis showed that Te doping led to the emergence of a large number of oxygen vacancies, which modulated the electronic structure of the crystal. It can be seen that the improvement of the catalytic performance is the result of the combined effect of the increase of active sites and oxygen vacancies.

In conclusion, Te doping is an effective method to obtain high-performance OER catalysts. Te element can be doped as either a cation or an anion in a catalyst, which can not only improve the OER kinetics, but also improve the catalyst stability.

2.2 Precious metal telluride catalysts

Noble metal catalysts are very efficient and stable OER catalytic materials. Most of the current state-of-the-art OER catalysts are Ir and Ru based materials, among which RuO_2 and IrO_2 are often used as benchmarks for OER catalysts [18, 84, 85]. Compared with non-noble metal catalysts, noble metal-based electrocatalysts are more efficient and stable under strongly acidic conditions, which makes them more suitable for proton exchange membrane (PEM) water electrolyzers [86–88]. PEM is considered to be the most promising practical application. However, the cost of precious metals is high. The introduction of Te element helps reduce the amount of precious metals used and is expected to improve catalyst performance.

Attaching noble metal catalysts to metallic Te is a good solution. In 2020, Xu, J. Y. et al. [89] prepared fine IrRu intermetallic nanoclusters (IrRu@Te) supported by amorphous Te nanoparticles via a one-pot hydrothermal method. The IrRu nanoclusters exhibited a large electrochemical specific surface area, while the Te nanoparticle supports exhibited high electrical conductivity of 606 S·cm^{-1} and good acid stability. DFT calculations showed that coupling the IrRu nanoclusters with Te changed the electronic structure of the IrRu nanoclusters, resulting in a shift of the density of states and the d-band center toward the Fermi level. As a result, IrRu@Te exhibited excellent OER catalytic performance, delivering current densities of 10 and 100 mA·cm^{-2} with 220 and 303 mV overpotentials, respectively, in a strongly acidic electrolyte of 0.5 M H_2SO_4. The Tafel slope was only 35 mV·dec^{-1}. Stability tests showed that IrRu@Te could sustain OER electricity for 20 h at 10 mA·cm^{-2}. XPS revealed that both IrRu nanoclusters and Te nanoparticles were oxidized during OER, but Te nanoparticles could help stabilize IrRu nanoclusters by inhibiting peroxidation and dissolution under corrosive and oxidative conditions.

Another promising solution to achieve high electrocatalytic OER efficiency is the preparation of 1D metal nanowires or nanotubes (NTs), which have high specific surface area, surface coordination unsaturation, and avoid the Ostwald ripening and possible occurrence of nanoparticles. The prevention of aggregation problem can not only expose more active sites, but also provide a pathway for fast electron transport rates [90–92]. In 2018, Shi, Q. R. et al. [93] first reported the facile synthesis of 1D hollow IrTe nanotubes with dendritic surfaces using ultrathin Te nanowires as a sacrificial template and a current displacement strategy at 190 °C. Under the acidic condition of 0.1 M $HClO_4$, the onset potential of IrTe nanotubes was 1.45 V, with a small overpotential of 290 mV and a Tafel slope of 60.3 mV·dec^{-1}. Moreover, it still exhibited strong structural stability and excellent electrocatalytic durability after 2,000 cycles of accelerated durability test, although most of the Ir on its surface had been oxidized to IrO_2 during the OER process. Under the neutral condition of 0.1 M phosphate-buffered saline (PBS) and the alkaline condition of 1 M KOH, the onset potentials of IrTe nanotubes were 1.44 and 1.45 V, respectively, and the overpotentials were lower than those of IrO_2. It can be seen that IrTe nanotubes are a novel class of materials with significantly enhanced electrocatalytic activity for OER over a wide pH range. Li, L. G. et al. [94] synthesized 1D Ir–Te nanowires, Ru–Te nanowires and Pt–Te nanowires using Te nanowires as templates (Fig. 2(a)). Among them, 1D porous Ir-Te nanowires exhibited the best OER activity with overpotentials of 248 and 284 mV at 10 mA·cm^{-2} in 1 M KOH (Fig. 2(b)) and 0.5 M H_2SO_4 (Fig. 2(c)), respectively. In 2022, Liu, M. et al. [95] synthesized ternary RuIrTe nanotubes by displacement reaction using pre-synthesized Te nanowires as starting materials (Fig. 2(d)). The modified catalyst exhibited high catalytic activity for total water splitting in the acidic environment of 0.5 M H_2SO_4, with overpotentials of 29 and

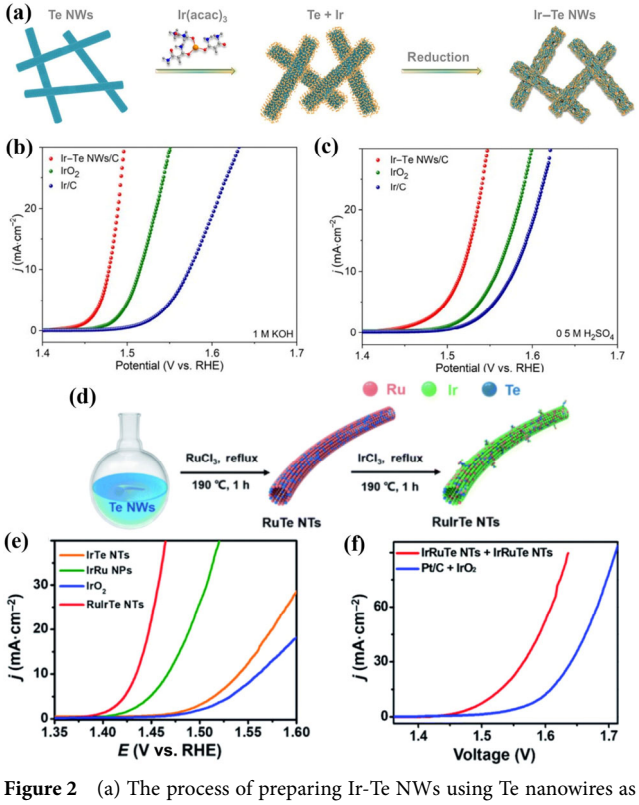

Figure 2 (a) The process of preparing Ir-Te NWs using Te nanowires as templates. (b) The LSV curves of the Ir-Te NWs/C, IrO_2 and Ir/C in 1 M KOH. (c) The LSV curves of the Ir-Te NWs/C, IrO_2 and Ir/C in 0.5 M H_2SO_4. (d) The process of preparing RuIrTe NTs. (e) The LSV curves of RuIrTe NTs in 0.5 M H_2SO_4. (f) The LSV curves of the water electrolyzer composed of RuIrTe NTs + RuIrTe NTs catalysts at a scan rate of 5 mV·s^{-1} in 0.5 M H_2SO_4. Panels (a)–(c): reproduced with permission from Ref. [94], © Tsinghua University Press and Springer-Verlag GmbH Germany, part of Springer Nature 2021. Panels (d)–(f): reproduced with permission from Ref. [95], © The Royal Society of Chemistry 2022.

205 mV for HER and OER, respectively (Fig. 2(e)). The two-electrode system assembled with RuIrTe nanotubes could reach a cell voltage of only 1.511 V at 10 mA·cm^{-2} (Fig. 2(f)). The main role of Te was to change the surface electronic properties of the catalyst, reduce the d-band center of Ir, optimize the adsorption energy of intermediate species, and improve the conductivity of the catalyst under acidic conditions.

$RuTe_2$ has also attracted the attention of researchers. In 2019, Wang, J. et al. [96] reported through theoretical calculations that the amorphous $RuTe_2$ system would exhibit a local distortion strain effect, allowing p-d electronic transitions that were forbidden in the original crystal structure to be allowed (Figs. 3(a) and 3(b)). This was conducive to local flexible bonding changes in Te coordination and induced mid- and long-range p–π coupling to effectively eliminate the Ru crystal field splitting effect and enhance intra-orbital and inter-orbital electron transfer (Fig. 3(c)), thereby improving the OER performance. They further calculated the bonding and antibonding orbitals near the Fermi level, demonstrating the p–π electron-rich nature of Te sites (Fig. 3(d)). This indicated that Te possessed high electron sensitivity to coupling O 2p orbitals for H_2O activation. Moreover, the short-range disorder promoted the strong electron–lattice coupling effect, which contributed to high OER activity under pH-universal conditions. They prepared crystalline and amorphous 1D nanorod-like $RuTe_2$ (Figs. 3(e) and 3(f)) and found that the overpotential of amorphous $RuTe_2$ was as low as 245 mV in 0.5 M H_2SO_4 (Fig. 3(g)) and 285 mV in 1 M KOH (Fig. 3(h)), which were much lower than those of crystalline $RuTe_2$. At the same time, amorphous $RuTe_2$ exhibited excellent corrosion resistance and stability. It did not change significantly within 24 h under strong acid conditions, and it could still maintain the amorphous structure. Electron paramagnetic resonance (EPR) and XPS tests showed that there were a large number of defects in the amorphous structure (Fig. 3(i)), which would be replaced by oxygen atoms to form RuO_xH_y to promote OER activity. In 2020, Tang, B. et al. [97] prepared super tiny $RuTe_2$ nanoparticles anchored on the graphene nanosheets with an

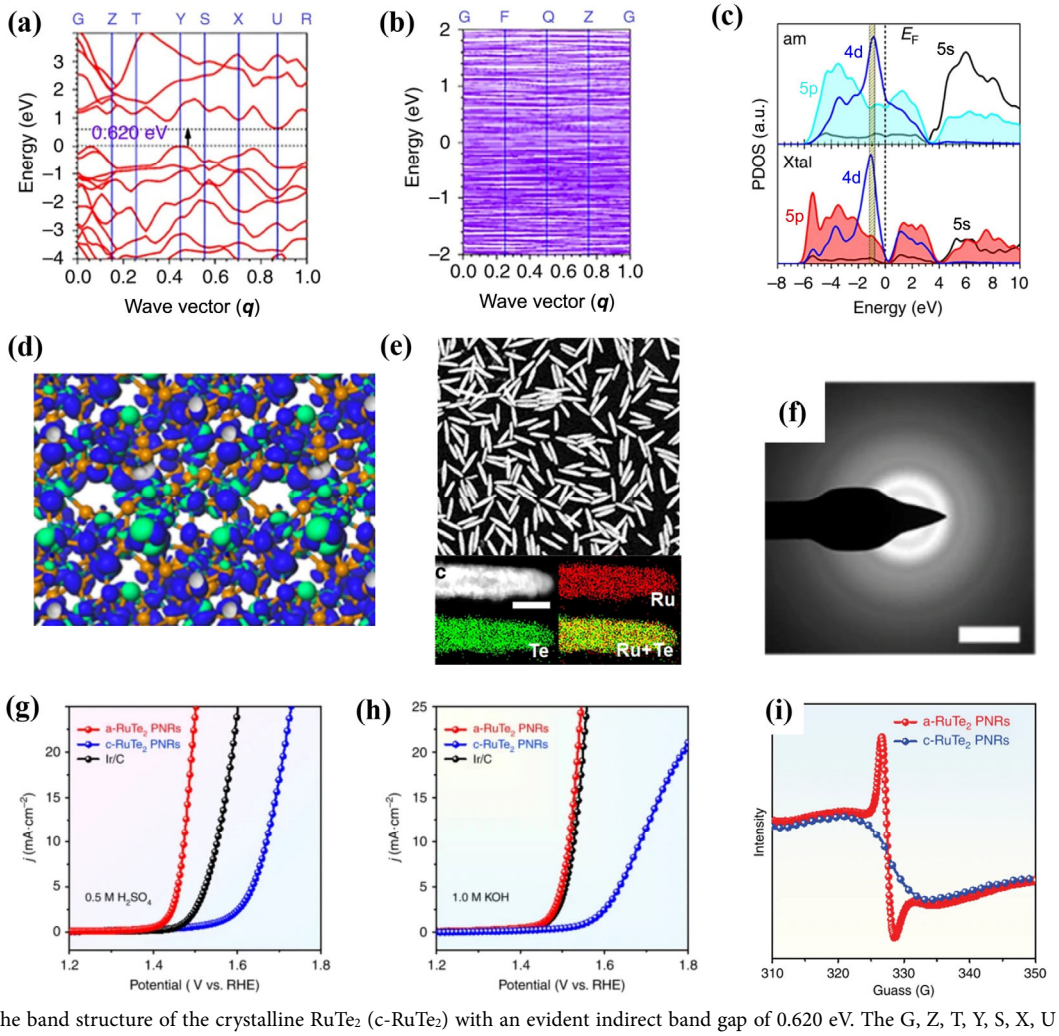

Figure 3 (a) The band structure of the crystalline $RuTe_2$ (c-$RuTe_2$) with an evident indirect band gap of 0.620 eV. The G, Z, T, Y, S, X, U and R denote high-symmetry points in the Brillouin zone. (b) The band structure of the amorphous $RuTe_2$ (a-$RuTe_2$) without any band gap. (c) The projected densities of states (PDOSs) of the crystalline (lower image) and amorphous (upper image) $RuTe_2$. The dotted line represents the Fermi level. (d) The real spatial contour plots for bonding and anti-bonding orbitals in $RuTe_2$ near E_F, demonstrating the p–π electron-rich nature of Te sites. (e) The high-angle annular dark-field scanning transmission electron microscopy (HAADF-STEM) image and energy-dispersive X-ray spectroscopy (EDS) elemental mappings of the $RuTe_2$. This demonstrates the successful preparation of $RuTe_2$ nanorods. (f) The selected area electron diffraction (SAED) pattern of $RuTe_2$, demonstrating that it is amorphous. (g) The LSV curves of the $RuTe_2$ in 0.5M H_2SO_4. (h) The LSV curves of the $RuTe_2$ in 1 M KOH. (i) The electron spin resonance (ESR) spectra of the $RuTe_2$, which reveals that there are a high density of defects in the a-$RuTe_2$. Panels (a)–(i): Reproduced with permission from Ref. [96], © Wang, J. et al. 2019.

average particle size of 2.9 ±0.2 nm. Benefiting from the high crystallinity, uniform distribution of nanoparticles and good electric conductivity, the HER and OER of $RuTe_2$ nanoparticles at a current density of 10 mA·cm^{-2} had small overpotentials of 34 and 275 mV, respectively, exhibiting a better performance than RuO_2. The catalyst was subjected to long-term water splitting electrolysis at the cell voltage of 2.00 V and current densities up to 100 mA cm^{-2}, showing excellent stability over a period of 20 h.

2.3 Transition metal telluride catalysts

Transition metal OER catalysts have always been the research focus [98]. Transition metal elements are abundant and inexpensive on earth, but they are criticized for the low activity and poor stability [99]. Recently, transition metal OER catalysts have demonstrated high OER activity, even surpassing the benchmark catalysts RuO_2 and IrO_2 [100, 101]. Among them, transition metal dichalcogenides have attracted great attention due to their outstanding mechanical and chemical stability, high abundance in the earth's crust, intrinsic semiconducting or metallic properties, and high catalytic efficiency [102–104]. They exhibit a layered structure that facilitates the preparation of 2D materials that expose more active sites. Additionally, they demonstrate two crystalline phases with completely different electronic structures (i.e., the semiconducting 2H phase and the metallic 1T phase) [105, 106]. The metallic 1T phase displays extraordinary electronic conductivity, facilitating the charge transfer process and possibly showing high activity in OER [107, 108]. Although there are few studies on transition metal tellurides, they have shown excellent OER activity and have huge development space and potential.

Among them, Fe, Co, and Ni have been widely studied because they are used as active sites and exhibit high OER activity [109–112]. The study of Co-Te compounds is firstly reported among them. In 2017, Gao, Q. et al. [113] first synthesized hierarchical $CoTe_2$ and CoTe nanofleeces using super tiny Te nanowires as templates (Fig. 4(a)). They exhibited excellent electrocatalytic OER activity and stability under alkaline conditions. $CoTe_2$ exhibited OER activity superior to CoTe, which is comparable to RuO_2 catalysts. In O_2-saturated 0.1 M KOH, the overpotential at a current density of 10 mA·cm^{-2} was about 357 mV (Fig. 4(b)), and the Tafel slope was about 32 mV·dec^{-1} (Fig. 4(c)). Majhi, K. C. et al. [114] constructed $CoTe_2$@CdTe nanocomposites by a hydrothermal method, which exhibited an ultra-low overpotential value of 140 mV and a Tafel slope value of 68 mV·dec^{-1} at 10 mA·cm^{-2}. The catalyst had good cycle stability, and no obvious change was observed after 500 cycles. It also exhibited high storage stability with almost negligible changes in the onset potential and current density after three months of storage. In 2020, Ji, L. L. et al. [115] prepared $Co_3[Co(CN)_6]_2$ nanocubes by a precipitation method, then chemically etched them in ammonia solution to obtain nanoframe structure, and finally carried out tellurization treatment to obtain $CoTe_2$. The overpotential of $CoTe_2$ nanoframes was 291 mV in 0.5 M H_2SO_4, and the Tafel slope was 78 mV·dec^{-1}. While in 1 M KOH, the overpotential was 302 mV, and the Tafel slope was 79.9 mV·dec^{-1}. Chen, Z. L. et al. [116] prepared N-doped hierarchically porous carbon and carbon nanotube-confined $CoTe_2$. They stimulated the structural transition of $CoTe_2$ from hexagonal to orthorhombic phase by P doping, which enhanced the OER activity, with an overpotential of only 241 mV at 10 mA·cm^{-2} in alkaline electrolyte and a high operational stability for 24 h. This phase transition not only allowed for more catalytically active site exposure and faster charge transfer, but also optimized the adsorption energy of the intermediate species. High-performance Co-Te catalysts were also obtained by Fe doping. He, B. et al. [117] prepared nitrogen-doped carbon nanotube frameworks encapsulated with different amounts of Fe dopants by chemical vapor deposition, using ZIF-67 with high surface area and porosity as Co precursor. $Co_{1.11}Te_2$ nanoparticles exhibited excellent OER performance at a current density of 10 mA·cm^{-2} with a minimum overpotential of 297 mV. In addition, the catalyst also exhibited promising HER performance. Using it as both the cathode and anode for overall water splitting could work stably for more than 20 h at a current density of 10 mA·cm^{-2}.

Ni-Te compounds have received more attention due to their excellent OER activity. In 2017, Bhat, K. S. et al. [118] first fabricated layered $Ni(OH)_2$ and chemically transformed it into porous hollow nickel telluride nanostructures through an anion exchange reaction under hydrothermal conditions. XRD showed that the catalyst had two phases, NiTe and $NiTe_2$. However, its OER performance was poor, with an overpotential of 679 mV and a Tafel slope of 151 mV·dec^{-1}. Masa, J. et al. [71] synthesized NiTe by a high temperature solid-state reaction with an overpotential of 400 mV. The activation energy at zero overpotential was revealed to be 100.2 kJ·mol^{-1} by the variable temperature linear sweep voltamperometry (LSV) test. Wang, Q et al. [119] synthesized NiTe domains on $Pb_{0.95}Ni_{0.05}Te$ nanorods by a two-step Te self-sacrificial template solvothermal method, which enhanced the OER activity of NiTe. Its overpotential was 387 mV at 10 mA·cm^{-2} and the Tafel slope was low in 1 M KOH solution, i.e., 96 mV·dec^{-1}, which were superior to those of pristine PbTe, NiTe and their powder mixtures. In 2018, De Silva, U. et al. [120] prepared Ni_3Te_2 by combining hydrothermal method and electrodeposition method, which exhibited ultra-high OER activity (Fig. 4(d)). Among them, Ni_3Te_2 prepared by electrodeposition had the best activity, affording a high current density of 10 mA·cm^{-2} with an overpotential of only 180 mV in alkaline electrolyte. This ultra-high activity was related to the crystal structure. It contained three crystallographically unique Ni sites: two tetrahedral Ni sites and one pyramidal Ni site, which may make the surface Ni site active easier and could better cover OH groups at low potentials, accelerating the OER process. Chronoamperometry studies were performed in 1 M KOH for 24 h at an applied voltage of 1.44 V, and no change in the current density was observed. The LSV curves before and after chronoamperometry did not show any difference in onset potential and overpotential (Fig. 4(e)). This meant that Ni_3Te_2 was very stable, and its surface oxidation was also stable during the OER process, and there was no conversion of oxide to oxyhydroxide. Fe doping can also enhance the OER activity. In 2021, Sadaqat, M. et al. [121] synthesized $Ni_{1-x}Fe_xTe_2$ nanoflakes on nickel foam by a facile hydrothermal method, requiring a low overpotential of only 190 and 274 mV to achieve 10 and 100 mA·cm^{-2}, respectively. The current density could be as high as 600 mA·cm^{-2} at an overpotential of 400 mV.

There are several studies on other transition element tellurides. The VTe_2 of the metal 1T phase is more stable than other vanadium-based dichalcogenides. In addition, it exhibits a charge density wave behavior. A large amount of charges can be transferred between the p-band of Te and the d-band of V, making 1T-VTe_2 more suitable for fast charge transfer reactions. Therefore, VTe_2 in the 1T phase is a promising highly active

OER catalyst. In 2022, Pan, U. N. et al. [122] prepared Ni nanocluster hybridization and Mn intercalation and doped 1T-VTe_2 nanosheets, which accomplished an overpotential of 258 mV at a current density of 40 mA·cm^{-2}. Zhang, W. Q. et al. [123] systematically studied the electronic structure and catalytic performance of transition metal monochalcogenide (MX, M = Cr, Mo, W; X = S, Se, Te) nanowires based on first-principles calculations. The results suggested that these MX nanowires could be regarded as efficient bifunctional catalysts for OER/ORR. The overpotentials of these MX nanowires ranged from 200 to 590 mV, which were comparable to or even better than the best-known OER catalyst RuO_2 (Fig. 4(f)). In particular, the CrTe nanowires were at the top of the OER volcano plot with the lowest overpotential of only 200 mV, which is 230 mV lower than that of $CrTe_2$ (Fig. 4(g)). Interestingly, positively charged metal sites were generally considered to be the active sites for OER and ORR in many electrocatalysts, but the metal atoms in MX nanowires were located in the core of the nanowire, which hindered the adsorption of intermediates and reduced their catalytic activity. Compared with the well-known transition metal dichalcogenide MX_2, the chalcogen atoms in MX were over-coordinated by four transition metal atoms, so they were more chemically active and could optimize the interaction with intermediates, serving as active sites to exhibit higher OER activity (Fig. 4(h)). The activities of Mo-based catalysts are far lower than those of the above-mentioned Co and Ni-based catalysts. But considering that Mo exists in the high-valence form Mo^{6+}, it is considered to possess high OER efficiency [124, 125]. In 2021, He, R. Z. et al. [126] grew Mo on the surface of Te nanorods to form a Te-Mo core–shell structure, but found that its stability was poor and its performance decayed during the activation. In order to solve this problem, the authors carried out Fe doping and successfully obtained the OER catalyst with high activity and long-term stability. When this catalyst was supported on a glassy carbon electrode, the overpotential at 10 mA·cm^{-2} was

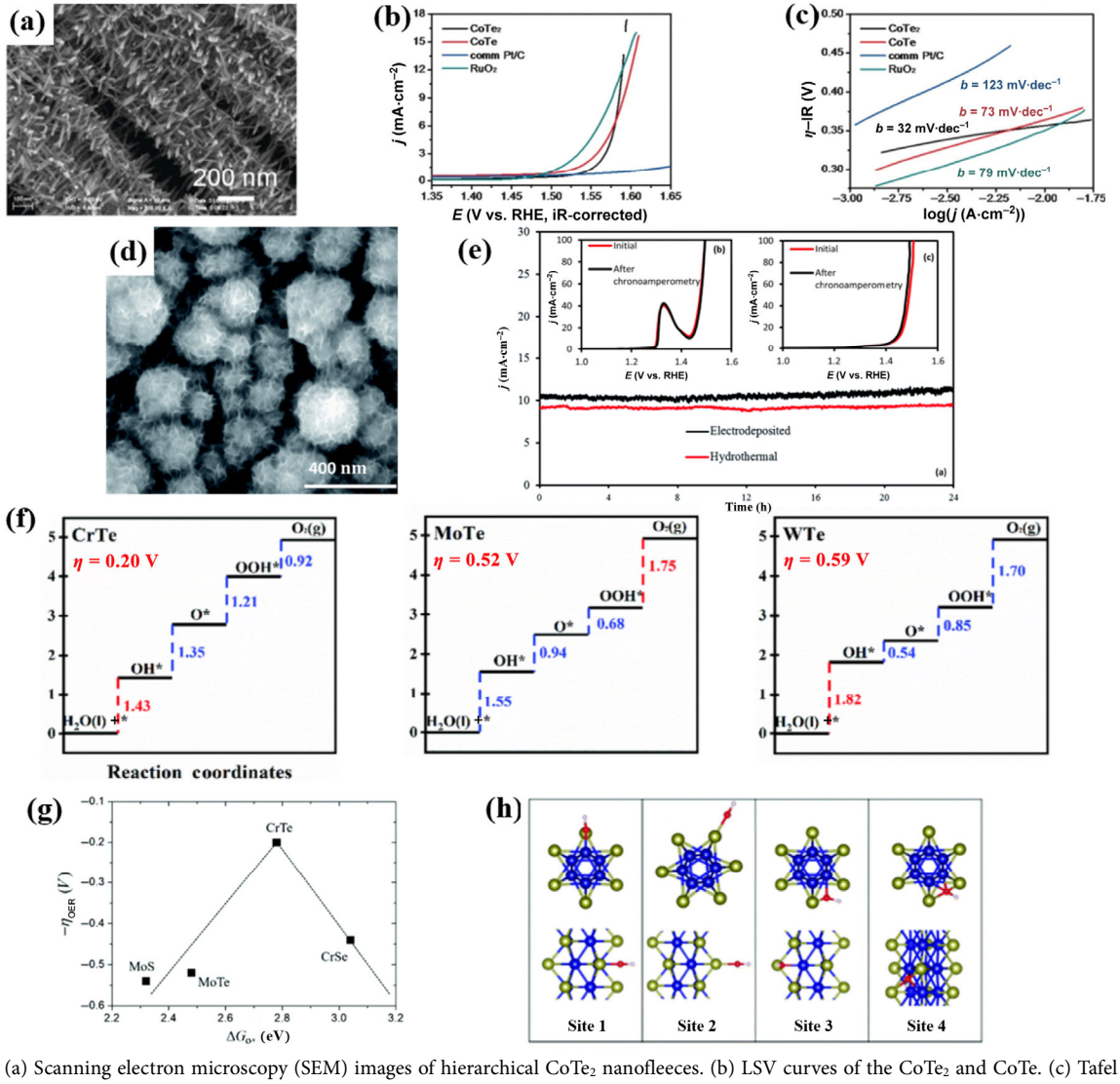

Figure 4 (a) Scanning electron microscopy (SEM) images of hierarchical $CoTe_2$ nanofleeces. (b) LSV curves of the $CoTe_2$ and CoTe. (c) Tafel slopes of the $CoTe_2$ and CoTe. (d) SEM images of Ni_3Te_2 composed of randomly oriented nanoflakes. (e) Stability study of the electrodeposited and hydrothermally synthesized Ni_3Te_2 through chronoamperometry at a constant potential of 1.44 and 1.45 V vs. RHE. (f) Electrochemical step diagram of CrTe, MoTe and WTe for OER process at zero potential. (g) The volcano plots of CrTe. (h) Possible adsorption sites for OH on double cell MX wires. Among them, blue balls represent metal atoms, yellow balls represent chalcogen atoms. Panels (a)–(c): reproduced with permission from Ref. [113], © Wiley-VCH Verlag GmbH & Co. KGaA, Weinheim 2017. Panels (d) and (e): reproduced with permission from Ref. [120], © The Royal Society of Chemistry 2018. Panels (f)–(h): reproduced with permission from Ref. [123], © The Royal Society of Chemistry 2020.

only 300 mV, which was about 140 mV lower than that without Fe doping. It displayed a low Tafel slope of 45.6 mV·dec^{-1} and a Faradaic efficiency close to 100%.

Bimetals can often produce synergistic effects to promote the OER process, and bimetallic tellurides similarly exhibit high OER activity [33, 127, 128]. In 2018, He, Q. et al. [129] developed a simple self-template method to construct Co-Sn-X (X = S, Se, Te) nanocages via an anion exchange reaction of $CoSn(OH)_6$. The Co-Sn-Te nanocages consisted of particles with a diameter of about 20 nm, with an overpotential of 343 mV and a Tafel slope of 91 mV·dec^{-1}. Majhi, K. C. et al. [130] synthesized nanorods Zn-Co-Te by a one-pot hydrothermal method with an OER onset potential of 1.38 V in KOH at pH = 15.14. It showed a low overpotential of 221 mV and the Tafel slope is 91 mV·dec^{-1} at a current density of 10 mA·cm^{-2}. It had high stability after 1,000 CV cycles and storage for three months. Qian, G. F. et al. [131] grew CoNi hydroxide on nickel foam by a hydrothermal method, followed by high-temperature tellurization to form bimetallic telluride $CoNiTe_2$. $CoNiTe_2$ exhibited higher catalytic activity than Ni, Co and CoNi. Its overpotential was 181 mV at 10 mA·cm^{-2}, 230 mV at 500 mA·cm^{-2}, and only 270 mV at 1,000 mA·cm^{-2}, with a low Tafel slope of 44 mV·dec^{-1}. The high activity may originate from two parts. (1) The flower-like structures were formed via the stacking of $CoNiTe_2$ nanosheets, which increased the specific surface area. (2) The Te element increased the covalency and reduced the electronegativity of the transition metal center anion network, thus further optimizing the electronic structure of the CoNi metal site and improving the catalytic activity.

3 Summary and outlook

In order to solve the increasingly urgent problems of energy shortage and environmental pollution, human beings need to find a new energy source to meet the needs of social development. Obtaining hydrogen energy from electrocatalytic water splitting is a very practical solution. But the OER process is kinetically limited. It is highly desirable to develop an efficient OER catalyst. Although a variety of noble metal-based and transition metal-based OER catalysts have been developed, there is still a lack of a catalyst with both high activity and high stability. Recently, chalcogenides become popular due to their ultra-high activity in OER. As an important member of chalcogens, Te element demonstrated the high activity and high stability in electrocatalytic OER, highlighting the great development potential. In this review, we outline its latest progress and further summarize it as follows.

Te element can be introduced into OER catalysts by doping and other methods to further improve catalysts with good electrocatalytic performance, such as 2D materials, MOF materials, and LDH materials. Due to the large radius of Te anion, it shows a huge impact on the lattice, including causing lattice distortions, reducing the crystal size, exposing more active sites, and changing the electronic structure of the crystal. Its incorporation can also lead to various intrinsic defects in the catalyst to form a more stable structure, and synergize with these defects to optimize the adsorption of intermediate species. Te has less electronegativity and can form strong covalent bonds with transition metals in catalysts, tune the d-band center, enhance the conductivity of catalysts, and facilitate charge transfer between adsorbed species and catalysts. At the same time, Te possesses a variety of coordination forms, so it is of key importance to stabilize the catalyst.

Compounds containing Te element show high activity in OER. Among them, noble metal tellurides display high OER activity in a wide pH range as well as good stability. Transition metal tellurides exhibit much lower overpotentials than oxides and also have good stability. The electrocatalytic performance of bimetallic tellurides is better, especially showing low overpotentials at high current densities. The main role of Te is to change the surface electronic properties of the catalyst, optimize the adsorption energy of intermediate species, and improve the conductivity of the catalyst. Amorphous tellurides demonstrate better properties than crystalline counterparts. The amorphous structures generate more defects. Moreover, the induced local distortion strain effects lead to changes in Te coordination, allowing the originally forbidden p–d transition process and therefore resulting in mid- and long-range p–π coupling and enhancing the electron transport process. Since the preparation method of Te nanowires is relatively mature, Te nanowires can be used as templates to prepare 1D nanowires and nanotubes. These structures have the characteristics of high specific surface area and surface coordination unsaturation, which greatly increases the number of active sites and further enhances the OER activity of tellurides. In addition, Te is also used as a substrate to support or grow nanomaterials. The interaction between Te and the supported nanomaterials can not only optimize the electronic structure to accelerate the OER process, but also help stabilize the nanomaterials by suppressing the peroxidation and dissolution processes.

Although Te-contained electrocatalysts are in their infancy of development, they have already served critical role in highly efficient OER reactions. As developing materials, they also have many problems and challenges as below.

First of all, the synthesis of nano-tellurides is difficult. Due to the small electronegativity of Te and its poor bonding ability, its chemical reactivity is low and it is usually difficult to form tellurides [132]. It is well known that air contains oxygen and Te is far less reactive than oxygen. When the chemical reactions happen in the air, they tend to obtain oxides rather than tellurides. Therefore, the precise control of the synthesis environment is required. Generally, there are several methods to craft nano-tellurides: (1) Solid-phase powders were sintered into crystals, and then the mechanical or chemical exfoliation was used to obtain nano-tellurides. But this method has low yield and is difficult to control the size [133]. (2) Nano-telluride thin films were grown by a chemical vapor deposition, but this route needs high energy consumption and achieve the poor uniformity of the products [134]. (3) Nano-tellurides were synthesized by a hydrothermal method, which can control the size and shape conveniently, but usually requires the participation of a strong reducing agent, such as hydrazine hydrate [135]. (4) Although homogeneous nano-tellurides can be obtained by an organic fabrication technique, the synthesize process is complex [136]. Therefore, it is necessary to find a facile, efficient and controllable approach to craft nano-tellurides.

Second, researches on defects are insufficient. Defects pose an intense influence on the properties of tellurides. For example, Fe as the cation doping and P as the anion doping enhance the activity and stability of tellurides, but there is a lack of comprehensive and systematic understanding of the mechanisms behind these defects. More experimental characterizations together with theoretical calculations are needed to conduct more in-depth studies on the chemical structure, formation mechanisms of defects and their effects on the catalytic activity and stability of catalysts.

Then, the mechanism by which Te enhances the OER activity of catalysts is not thorough, and there is a lack of researches on the chemical behavior of Te element during the OER process. In the future, *in-situ* characterization methods, such as *in-situ* Raman spectroscopy and *in-situ* XRD, should be used to characterize materials in the OER process and analyze the role of Te element. At the same time, more first-principles calculations should be conducted on tellurides, which are analyzed from the perspectives of electronic structure and adsorption energy.

The mechanism by which Te enhances catalyst stability is lacking. Te is an element that is easily oxidized, and the change of the valence state of Te is also observed in the experiment. But there is still no reasonable explanation why this can still maintain the high activity of the catalyst. Considering Te has various oxidation states, it is necessary to study the Pourbaxi diagram of telluride to explore its possible stable forms at different potentials.

It is worth noting that Te has toxicity and can threaten the human health. Therefore, it is necessary to conduct more detailed research on the behavior of Te element in the catalysts, especially the phase change of Te element during the catalytic process and the dissolution behavior of Te element. This research will also advance the understanding on the stability of Te-containing catalysts.

There are few studies on electrocatalytic performance of Te-contained electrocatalysts at high current density. In practical applications, it needs to be carried out at high current density. Therefore, the study of catalyst behavior at high current density is more conducive to solving practical energy problems.

In view of the remarkable performance of binary metal tellurides, the research on these materials should be increased. Considering the high-entropy effect of current oxide OER catalysts, multi-metal tellurides should be investigated, which may further improve the OER performance. Meanwhile, considering the ultra-high activity exhibited by current single-atom catalysts and covalent organic framework (COF) catalysts, it is necessary to study similar tellurium-based catalysts [137–140].

Acknowledgements

M. Y. W. gratefully acknowledges the financial support from the National Natural Science Foundation of China (No. 21905317) and the Young Elite Scientists Sponsorship Program by CAST (No. 2019QNRC001).

Declaration of conflicting interests

The authors declare no conflicting interests regarding the content of this article.

References

[1] Chu, S.; Majumdar, A. Opportunities and challenges for a sustainable energy future. *Nature* **2012**, *488*, 294–303.

[2] Capellán-Pérez, I.; Mediavilla, M.; de Castro, C.; Carpintero, Ó.; Miguel, L. J. Fossil fuel depletion and socio-economic scenarios: An integrated approach. *Energy* **2014**, *77*, 641–666.

[3] Dresselhaus, M. S.; Thomas, I. L. Alternative energy technologies. *Nature* **2001**, *414*, 332–337.

[4] Lewis, N. S.; Nocera, D. G. Powering the planet: Chemical challenges in solar energy utilization. *Proc. Natl. Acad. Sci. USA* **2006**, *103*, 15729–15735.

[5] Wang, S. Q.; Tian, C. Z.; Zhou, P.; Zou, L. Q. Grid energy efficiency assessment considering intermittent new energy. In *International Conference on Advanced Materials and Energy Sustainability (AMES)*, World Scientific Publ Co Pte Ltd., Wuhan, China, 2016, pp 362–367.

[6] Moriarty, P.; Honnery, D. Can renewable energy power the future?. *Energy Policy* **2016**, *93*, 3–7.

[7] Xiong, X. H.; Yang, C. H.; Wang, G. H.; Lin, Y. W.; Ou, X.; Wang, J. H., Zhao, B. T.; Liu, M. L.; Lin, Z.; Huang, K. SnS nanoparticles electrostatically anchored on three-dimensional N-doped graphene as an active and durable anode for sodium-ion batteries. *Energy Environ. Sci.* **2017**, *10*, 1757–1763.

[8] Yang, B. P.; Liu, K.; Li, H. J. W.; Liu, C. X.; Fu, J. W.; Li, H. M.; Huang, J. E.; Ou, P. F.; Alkayyali, T.; Cai, C. et al. Accelerating CO_2 electroreduction to multicarbon products via synergistic electric-thermal field on copper nanoneedles. *J. Am. Chem. Soc.* **2022**, *144*, 3039–3049.

[9] Song, H.; Ou, X. W.; Han, B.; Deng, H. Y.; Zhang, W. C.; Tian, C.; Cai, C. F.; Lu, A. H.; Lin, Z.; Chai, L. Y. An overlooked natural hydrogen evolution pathway: Ni^{2+} boosting H_2O reduction by $Fe(OH)_2$ oxidation during low-temperature serpentinization. *Angew. Chem., Int. Ed.* **2021**, *60*, 24054–24058.

[10] Ye, X. C.; Lin, Z. H.; Liang, S. J.; Huang, X. H.; Qiu, X. Y.; Qiu, Y. C.; Liu, X. M.; Xie, D.; Deng, H.; Xiong, X. H. et al. Upcycling of electroplating sludge into ultrafine Sn@C nanorods with highly stable lithium storage performance. *Nano Lett.* **2019**, *19*, 1860–1866.

[11] Steele, B. C. H.; Heinzel, A. Materials for fuel-cell technologies. *Nature* **2001**, *414*, 345–352.

[12] Schlapbach, L.; Züttel, A. Hydrogen-storage materials for mobile applications. *Nature* **2001**, *414*, 353–358.

[13] Bockris, J. O. M. Hydrogen no longer a high cost solution to global warming: New ideas. *Int. J. Hydrogen Energy* **2008**, *33*, 2129–2131.

[14] Suen, N. T.; Hung, S. F.; Quan, Q.; Zhang N.; Xu, Y. J.; Chen, H. M. Electrocatalysis for the oxygen evolution reaction: Recent development and future perspectives. *Chem. Soc. Rev.* **2017**, *46*, 337–365.

[15] Koper, M. T. M. Thermodynamic theory of multi-electron transfer reactions: Implications for electrocatalysis. *J. Electroanal. Chem.* **2011**, *660*, 254–260.

[16] Sun, H. N.; Xu, X. M.; Song, Y. F.; Zhou, W.; Shao, Z. P. Designing high-valence metal sites for electrochemical water splitting. *Adv. Funct. Mater.* **2021**, *31*, 2009779.

[17] Rossmeisl, J.; Qu, Z. W.; Zhu, H.; Kroes, G. J.; Nørskov, J. K. Electrolysis of water on oxide surfaces. *J. Electroanal. Chem.* **2007**, *607*, 83–89.

[18] Lee, Y.; Suntivich, J.; May, K. J.; Perry, E. E.; Shao-Horn, Y. Synthesis and activities of rutile IrO_2 and RuO_2 nanoparticles for oxygen evolution in acid and alkaline solutions. *J. Phys. Chem. Lett.* **2012**, *3*, 399–404.

[19] Subbaraman, R.; Tripkovic, D.; Chang, K. C.; Strmcnik, D.; Paulikas, A. P.; Hirunsit, P.; Chan, M.; Greeley, J.; Stamenkovic, V.; Markovic, N. M. Trends in activity for the water electrolyser reactions on 3d M(Ni, Co, Fe, Mn) hydr(oxy)oxide catalysts. *Nat. Mater.* **2012**, *11*, 550–557.

[20] Zhang, J. Y.; Bai, X. W.; Wang, T. T.; Xiao, W.; Xi, P. X.; Wang, J. L.; Gao, D. Q.; Wang, J. Bimetallic nickel cobalt sulfide as efficient electrocatalyst for Zn-air battery and water splitting. *Nano-Micro Lett.* **2019**, *11*, 2.

[21] Du, J.; Zou, Z. H.; Liu, C.; Xu, C. L. Hierarchical Fe-doped Ni_3Se_4 ultrathin nanosheets as an efficient electrocatalyst for oxygen evolution reaction. *Nanoscale* **2018**, *10*, 5163–5170.

[22] Liu, K. W.; Zhang, C. L.; Sun, Y. D.; Zhang, G. H.; Shen, X. C.; Zou, F.; Zhang, H. C.; Wu, Z. W.; Wegener, E. C.; Taubert, C. J. et al. High-performance transition metal phosphide alloy catalyst for oxygen evolution reaction. *ACS Nano* **2018**, *12*, 158–167.

[23] Duan, S.; Chen, S.; Wang, T.; Li, S.; Liu, J.; Liang, J.; Xie, H.; Han, J.; Jiao, S.; Cao, R. et al. Elemental selenium enables enhanced water oxidation electrocatalysis of NiFe layered double hydroxides. *Nanoscale* **2019**, *11*, 17376–17383.

[24] Chen, J. W.; Zhang, T.; Wang, J. L.; Xu, L.; Lin, Z. Y.; Liu, J. D.; Wang, C.; Zhang, N.; Lau, S. P.; Zhang, W. J. et al. Topological phase change transistors based on tellurium Weyl semiconductor. *Sci. Adv.* **2022**, *8*, eabn3837.
[25] Xue, X. X.; Feng, Y. X.; Liao, L.; Chen, Q. J.; Wang, D.; Tang, L. M.; Chen, K. Q. Strain tuning of electronic properties of various dimension elemental tellurium with broken screw symmetry. *J. Phys.: Condens. Matter* **2018**, *30*, 125001.
[26] Lin, Z. Y.; Wang, J. L.; Chen, J. W.; Wang, C.; Liu, J. D.; Zhang, W. J.; Chai, Y. Two-dimensional tellurene transistors with low contact resistance and self-aligned catalytic thinning process. *Adv. Electron. Mater.*, in press, https://doi.org/10.1002/aelm.202200380.
[27] Qiu, B.; Wang, C.; Wang, J.; Lin, Z.; Zhang, N.; Cai, L.; Tao, X.; Chai, Y. Metal-free tellurene cocatalyst with tunable bandgap for enhanced photocatalytic hydrogen production. *Mater. Today Energy* **2021**, *21*, 100720.
[28] Rasmussen, F. A.; Thygesen, K. S. Computational 2D materials database: Electronic structure of transition-metal dichalcogenides and oxides. *J. Phys. Chem. C* **2015**, *119*, 13169–13183.
[29] Masud, J.; Ioannou, P. C.; Levesanos, N.; Kyritsis, P.; Nath, M. A molecular Ni-complex containing tetrahedral nickel selenide core as highly efficient electrocatalyst for water oxidation. *ChemSusChem* **2016**, *9*, 3128–3132.
[30] Liang, Q. H.; Brocks, G.; Sinha, V.; Bieberle-Hütter, A. Tailoring the performance of ZnO for oxygen evolution by effective transition metal doping. *ChemSusChem* **2021**, *14*, 3064–3073.
[31] Zhu, K. Y.; Zhu, X. F.; Yang, W. S. Application of *in situ* techniques for the characterization of NiFe-based oxygen evolution reaction (OER) electrocatalysts. *Angew. Chem., Int. Ed.* **2019**, *58*, 1252–1265.
[32] Fan, K.; Zou, H. Y.; Lu, Y.; Chen, H.; Li, F. S.; Liu, J. X.; Sun, L. C.; Tong, L. P.; Toney, M. F.; Sui, M. L. et al. Direct observation of structural evolution of metal chalcogenide in electrocatalytic water oxidation. *ACS Nano* **2018**, *12*, 12369–12379.
[33] Zhao, J.; He, X. Y. Preparation and electrocatalytic properties of oxygen precipitation of amorphous NiCo oxide. *J. Synth. Cryst.* **2020**, *49*, 896–901, 907.
[34] Diao, J. X.; Qiu, Y.; Guo, X. H. Synthesis of mesoporous Co_3S_4 nanorods and their application as electrocatalysts for efficient oxygen evolution. *J. Synth. Cryst.* **2018**, *47*, 370–373, 381.
[35] Dionigi, F.; Zeng, Z. H.; Sinev, I.; Merzdorf, T.; Deshpande, S.; Lopez, M. B.; Kunze, S.; Zegkinoglou, I.; Sarodnik, H.; Fan, D. X. et al. *In-situ* structure and catalytic mechanism of NiFe and CoFe layered double hydroxides during oxygen evolution. *Nat. Commun.* **2020**, *11*, 2522.
[36] Liu, Y. P.; Liang, X.; Gu, L.; Zhang, Y.; Li, G. D.; Zou, X. X.; Chen, J. S. Corrosion engineering towards efficient oxygen evolution electrodes with stable catalytic activity for over 6,000 hours. *Nat. Commun.* **2018**, *9*, 2609.
[37] Long, X.; Li, J. K.; Xiao, S.; Yan, K. Y.; Wang, Z. L.; Chen, H. N.; Yang, S. H. A strongly coupled graphene and FeNi double hydroxide hybrid as an excellent electrocatalyst for the oxygen evolution reaction. *Angew. Chem., Int. Ed.* **2014**, *53*, 7584–7588.
[38] Peng, C. L.; Ran, N.; Wan, G.; Zhao, W. P.; Kuang, Z. Y.; Lu, Z.; Sun, C. J.; Liu, J. J.; Wang, L. Z.; Chen, H. R. Engineering active Fe sites on nickel-iron layered double hydroxide through component segregation for oxygen evolution reaction. *ChemSusChem* **2020**, *13*, 811–818.
[39] Mishra, A. K.; Pradhan, D. Hierarchical urchin-like cobalt-doped CuO for enhanced electrocatalytic oxygen evolution reaction. *ACS Appl. Energy Mater.* **2021**, *4*, 9412–9419.
[40] Xiong, X. L.; You, C.; Liu, Z. A.; Asiri, A. M.; Sun, X. P. Co-doped CuO nanoarray: An efficient oxygen evolution reaction electrocatalyst with enhanced activity. *ACS Sustainable Chem. Eng.* **2018**, *6*, 2883–2887.
[41] Kim, G. H.; Park, Y. S.; Yang, J. C.; Jang, M. J.; Jeong, J.; Lee, J. H.; Park, H. S.; Park, Y. H.; Choi, S. M.; Lee, J. Effects of annealing temperature on the oxygen evolution reaction activity of copper-cobalt oxide nanosheets. *Nanomaterials* **2021**, *11*, 657.
[42] Nguyen, T. X.; Liao, Y. C.; Lin, C. C.; Su, Y. H.; Ting, J. M. Advanced high entropy perovskite oxide electrocatalyst for oxygen evolution reaction. *Adv. Funct. Mater.* **2021**, *31*, 2101632.
[43] Wang, T.; Chen, H.; Yang, Z. Z.; Liang, J. Y.; Dai, S. High-entropy perovskite fluorides: A new platform for oxygen evolution catalysis. *J. Am. Chem. Soc.* **2020**, *142*, 4550–4554.
[44] Zhang, J.; Quast, T.; He, W. H.; Dieckhöfer, S.; Junqueira, J. R. C.; Öhl, D.; Wilde, P.; Jambrec, D.; Chen, Y. T.; Schuhmann, W. *In situ* carbon corrosion and Cu leaching as a strategy for boosting oxygen evolution reaction in multimetal electrocatalysts. *Adv. Mater.* **2022**, *34*, 2109108.
[45] Chen, K. J.; Liu, K.; An, P. D.; Li, H. J. W.; Lin, Y. Y.; Hu, J. H.; Jia, C. K.; Fu, J. W.; Li, H. M.; Liu, H. et al. Iron phthalocyanine with coordination induced electronic localization to boost oxygen reduction reaction. *Nat. Commun.* **2020**, *11*, 4173.
[46] Shanthi, N.; Mahadevan, P.; Sarma, D. D. Electronic band structure of cadmium chromium chalcogenide spinels: $CdCr_2S_4$ and $CdCr_2Se_4$. *J. Solid State Chem.* **2000**, *155*, 198–205.
[47] Zhang, J. J.; Wu, M. H.; Shi, Z. T.; Jiang, M.; Jian, W. J.; Xiao, Z. R.; Li, J. X.; Lee, C. S.; Xu, J. Composition and interface engineering of alloyed $MoS_{2x}Se_{2(1-x)}$ nanotubes for enhanced hydrogen evolution reaction activity. *Small* **2016**, *12*, 4379–4385.
[48] Cai, P. W.; Huang, J. H.; Chen, J. X.; Wen, Z. H. Oxygen-containing amorphous cobalt sulfide porous nanocubes as high-activity electrocatalysts for the oxygen evolution reaction in an alkaline/neutral medium. *Angew. Chem., Int. Ed.* **2017**, *56*, 4858–4861.
[49] Zhang, H. B.; Zhou, W.; Dong, J. C.; Lu, X. F.; Lou, X. W. Intramolecular electronic coupling in porous iron cobalt (oxy)phosphide nanoboxes enhances the electrocatalytic activity for oxygen evolution. *Energy Environ. Sci.* **2019**, *12*, 3348–3355.
[50] Wang, Y.; Li, X. P.; Zhang, M. M.; Zhang, J. F.; Chen, Z. L.; Zheng, X. R.; Tian, Z. L.; Zhao, N. Q.; Han, X. P.; Zaghib, K. et al. Highly active and durable single-atom tungsten-doped $NiS_{0.5}Se_{0.5}$ nanosheet@$NiS_{0.5}Se_{0.5}$ nanorod heterostructures for water splitting. *Adv. Mater.* **2022**, *34*, 2107053.
[51] Acharya, P.; Manso, R. H.; Hoffman, A. S.; Bakovic, S. I. P.; Kékedy-Nagy, L.; Bare, S. R.; Chen, J. Y.; Greenlee, L. F. Fe coordination environment, Fe-Incorporated $Ni(OH)_2$ phase, and metallic core are key structural components to active and stable nanoparticle catalysts for the oxygen evolution reaction. *ACS Catal.* **2022**, *12*, 1992–2008.
[52] Jin, Y. S.; Huang, S. L.; Yue, X.; Du, H. Y.; Shen, P. K. Mo- and Fe-modified $Ni(OH)_2$/NiOOH nanosheets as highly active and stable electrocatalysts for oxygen evolution reaction. *ACS Catal.* **2018**, *8*, 2359–2363.
[53] Yan, J. Q.; Kong, L. Q.; Ji, Y. J.; White, J.; Li, Y. Y.; Zhang, J.; An, P. F.; Liu, S. Z.; Lee, S. T.; Ma, T. Y. Single atom tungsten doped ultrathin α-$Ni(OH)_2$ for enhanced electrocatalytic water oxidation. *Nat. Commun.* **2019**, *10*, 2149.
[54] Han, G. F.; Li, F.; Rykov, A. I.; Im, Y. K.; Yu, S. Y.; Jeon, J. P.; Kim, S. J.; Zhou, W. H.; Ge, R. L.; Ao, Z. M. et al. Abrading bulk metal into single atoms. *Nat. Nanotechnol.* **2022**, *17*, 403–407.
[55] Qiao, J. S.; Kong, X. H.; Hu, Z. X.; Yang, F.; Ji, W. High-mobility transport anisotropy and linear dichroism in few-layer black phosphorus. *Nat. Commun.* **2014**, 5, 4475.
[56] Pang, X.; Xue, S. X.; Zhou, T.; Yuan, H. D.; Liu, C.; Lei, W. Y. Advances in two-dimensional black phosphorus-based nanostructures for photocatalytic applications. *Prog. Chem.* **2022**, *34*, 630–642.
[57] Eswaraiah, V.; Zeng, Q. S.; Long, Y.; Liu, Z. Black phosphorus nanosheets: Synthesis, characterization and applications. *Small* **2016**, *12*, 3480–3502.
[58] Flores, E.; Ares, J. R.; Castellanos-Gomez, A.; Barawi, M.; Ferrer, I. J.; Sánchez, C. Thermoelectric power of bulk black-phosphorus. *Appl. Phys. Lett.* **2015**, *106*, 022102.
[59] Guo, Q. S.; Pospischil, A.; Bhuiyan, M.; Jiang, H.; Tian, H.; Farmer, D.; Deng, B. C.; Li, C.; Han, S. J.; Wang, H. et al. Black phosphorus mid-infrared photodetectors with high gain. *Nano Lett.* **2016**, *16*, 4648–4655.
[60] Zeng, L.; Zhang, X.; Liu, Y. N.; Yang, X. X.; Wang, J. H.; Liu, Q.;

Luo, Q.; Jing, C. Y.; Yu, X. F.; Qu, G. B. et al. Surface and interface control of black phosphorus. *Chem* **2022**, *8*, 632–662.
[61] Yang, B. C.; Wan, B. S.; Zhou, Q. H.; Wang, Y.; Hu, W. T.; Lv, W. M.; Chen, Q.; Zeng, Z. M.; Wen, F. S.; Xiang, J. Y. et al. Te-doped black phosphorus field-effect transistors. *Adv. Mater.* **2016**, *28*, 9408–9415.
[62] Zhang, Z. M.; Khurram, M.; Sun, Z. J.; Yan, Q. F. Uniform tellurium doping in black phosphorus single crystals by chemical vapor transport. *Inorg. Chem.* **2018**, *57*, 4098–4103.
[63] Zhu, J. F.; Jiang, X. X.; Yang, Y.; Chen, Q. J.; Xue, X. X.; Chen, K. Q.; Feng, Y. X. Synergy of tellurium and defects in control of activity of phosphorene for oxygen evolution and reduction reactions. *Phys. Chem. Chem. Phys.* **2019**, *21*, 22939–22946.
[64] Mou, Q. X.; Xu, Z. H.; Wang, G. N.; Li, E. L.; Liu, J. Y.; Zhao, P. P.; Liu, X. H.; Li, H. B.; Cheng, G. Z. A bimetal hierarchical layer structure MOF grown on Ni foam as a bifunctional catalyst for the OER and HER. *Inorg. Chem. Front.* **2021**, *8*, 2889–2899.
[65] Park, K.; Kwon, J.; Jo, S.; Choi, S.; Enkhtuvshin, E.; Kim, C.; Lee, D.; Kim, J.; Sun, S.; Han, H. et al. Simultaneous electrical and defect engineering of nickel iron metal-organic-framework via co-doping of metalloid and non-metal elements for a highly efficient oxygen evolution reaction. *Chem. Eng. J.* **2022**, *439*, 135720.
[66] Hu, C. S.; Chen, J.; Wang, Y. Q.; Huang, Y.; Wang, S. T. A telluride-doped porous carbon as highly efficient bifunctional catalyst for rechargeable Zn-air batteries. *Electrochim. Acta* **2022**, *404*, 139606.
[67] Yang, Y.; Dang, L. N.; Shearer, M. J.; Sheng, H. Y.; Li, W. J.; Chen, J.; Xiao, P.; Zhang, Y. H.; Hamers, R. J.; Jin, S. Highly active trimetallic NiFeCr layered double hydroxide electrocatalysts for oxygen evolution reaction. *Adv. Energy Mater.* **2018**, *8*, 1703189.
[68] Gao, R.; Yan, D. P. Fast formation of single-unit-cell-thick and defect-rich layered double hydroxide nanosheets with highly enhanced oxygen evolution reaction for water splitting. *Nano Res.* **2018**, *11*, 1883–1894.
[69] Chen, R.; Hung, S. F.; Zhou, D. J.; Gao, J. J.; Yang, C. J.; Tao, H. B.; Yang, H. B.; Zhang, L. P.; Zhang, L. L.; Xiong, Q. H. et al. Layered structure causes bulk NiFe layered double hydroxide unstable in alkaline oxygen evolution reaction. *Adv. Mater.* **2019**, *31*, 1903909.
[70] Guo, F. F.; Wu, Y. Y.; Chen, H.; Liu, Y. P.; Yang, L.; Ai, X.; Zou, X. X. High-performance oxygen evolution electrocatalysis by boronized metal sheets with self-functionalized surfaces. *Energy Environ. Sci.* **2019**, *12*, 684–692.
[71] Masa, J.; Piontek, S.; Wilde, P.; Antoni, H.; Eckhard, T.; Chen, Y. T.; Muhler, M.; Apfel, U. P.; Schuhmann, W. Ni-metalloid (B, Si, P, As, and Te) alloys as water oxidation electrocatalysts. *Adv. Energy Mater.* **2019**, *9*, 1900796.
[72] Han, H.; Kim, K. M.; Ryu, J. H.; Lee, H. J.; Woo, J.; Ali, G.; Chung, K. Y.; Kim, T.; Kang, S.; Choi, S. et al. Boosting oxygen evolution reaction of transition metal layered double hydroxide by metalloid incorporation. *Nano Energy* **2020**, *75*, 104945.
[73] Lee, J. I.; Chae, H. R.; Ryu, J. H. Tellurium-incorporated nickel-cobalt layered double hydroxide and its oxygen evolution reaction. *Korean J. Met. Mater.* **2021**, *59*, 491–498.
[74] Lee, J. I.; Oh, S. G.; Kim, Y. J.; Park, S. J.; Sin, G. S.; Kim, J. H.; Ryu, J. H. Electrocatalytic properties of Te incorporated $Ni(OH)_2$ microcrystals grown on Ni foam. *J. Korean Cryst. Growth Cryst. Technol.* **2021**, *31*, 96–101.
[75] Masa, J.; Sinev, I.; Mistry, H.; Ventosa, E.; de la Mata, M.; Arbiol, J.; Muhler, M.; Roldan Cuenya, B.; Schuhmann, W. Ultrathin high surface area nickel boride (Ni_xB) nanosheets as highly efficient electrocatalyst for oxygen evolution. *Adv. Energy Mater.* **2017**, *7*, 1700381.
[76] Li, X. Y.; Yu, L.; Wang, G. L.; Wan, G. P.; Peng, X. G.; Wang, K.; Wang, G. Z. Hierarchical NiAl LDH nanotubes constructed via atomic layer deposition assisted method for high performance supercapacitors. *Electrochim. Acta* **2017**, *255*, 15–22.
[77] Chen, Y. Z.; Pang, W. K.; Bai, H. H.; Zhou, T. F.; Liu, Y. N.; Li, S.; Guo, Z. P. Enhanced structural stability of nickel-cobalt hydroxide via intrinsic pillar effect of metaborate for high-power and long-life supercapacitor electrodes. *Nano Lett.* **2017**, *17*, 429–436.
[78] Lee, S. Y.; Kim, I. S.; Cho, H. S.; Kim, C. H.; Lee, Y. K. Resolving potential-dependent degradation of electrodeposited $Ni(OH)_2$ catalysts in alkaline oxygen evolution reaction (OER): *In situ* XANES studies. *Appl. Catal. B* **2021**, *284*, 119729.
[79] Zhang, D.; Tang, X. N.; Yang, Z. G.; Yang, Y.; Li, H. P. Construction of honeycomb-like Te-doped NiCo-LDHs for aqueous supercapacitors and as oxygen evolution reaction electrocatalysts. *Mater. Adv.* **2022**, *3*, 1286–1294.
[80] Wang, Y.; Liu, L.; Wang, Y. W.; Fang, L.; Wan, F.; Zhang, H. J. Constituent-tunable ternary $CoM_{2x}Se_{2(1-x)}$ (M = Te, S) sandwich-like graphitized carbon-based composites as highly efficient electrocatalysts for water splitting. *Nanoscale* **2019**, *11*, 6108–6119.
[81] Ibraheem, S.; Li, X. T.; Shah, S. S. A.; Najam, T.; Yasin, G.; Iqbal, R.; Hussain, S.; Ding, W. Y.; Shahzad, F. Tellurium triggered formation of Te/Fe-NiOOH nanocubes as an efficient bifunctional electrocatalyst for overall water splitting. *ACS Appl. Mater. Interfaces* **2021**, *13*, 10972–10978.
[82] Wu, X. J.; Lu, L. J.; Liu, H. Z.; Feng, L.; Li, W. J.; Sun, L. C. Metalloid Te-doped fe-based catalysts applied for electrochemical water oxidation. *ChemistrySelect* **2021**, *6*, 6154–6158.
[83] Li, G. R.; Yu, X. T.; Yin, F. X.; Lei, Z. P.; Zhao, X. R.; He, X. B.; Li, Z. C. High-performance Te-doped Co_3O_4 nanocatalysts for oxygen evolution reaction. *Int. J. Energy Res.* **2022**, *46*, 5963–5972.
[84] Over, H. Fundamental studies of planar single-crystalline oxide model electrodes (RuO_2, IrO_2) for acidic water splitting. *ACS Catal.* **2021**, *11*, 8848–8871.
[85] Ma, Z.; Zhang, Y.; Liu, S. Z.; Xu, W. Q.; Wu, L. J.; Hsieh, Y. C.; Liu, P.; Zhu, Y. M.; Sasaki, K.; Renner, J. N. et al. Reaction mechanism for oxygen evolution on RuO_2, IrO_2, and RuO_2@IrO_2 core–shell nanocatalysts. *J. Electroanal. Chem.* **2018**, *819*, 296–305.
[86] Zhang, R. H.; Dubouis, N.; Ben Osman, M.; Yin, W.; Sougrati, M. T.; Corte, D. A. D.; Giaume, D.; Grimaud, A. A dissolution/precipitation equilibrium on the surface of iridium-based perovskites controls their activity as oxygen evolution reaction catalysts in acidic media. *Angew. Chem., Int. Ed.* **2019**, *58*, 4571–4575.
[87] Gao, R. Q.; Zhang, Q.; Chen, H.; Chu, X. F.; Li, G. D.; Zou, X. X. Efficient acidic oxygen evolution reaction electrocatalyzed by iridium-based 12L-perovskites comprising trinuclear face-shared IrO_6 octahedral strings. *J. Energy Chem.* **2020**, *47*, 291–298.
[88] McCrory, C. C. L.; Jung, S.; Ferrer, I. M.; Chatman, S. M.; Peters, J. C.; Jaramillo, T. F. Benchmarking hydrogen evolving reaction and oxygen evolving reaction electrocatalysts for solar water splitting devices. *J. Am. Chem. Soc.* **2015**, *137*, 4347–4357.
[89] Xu, J. Y.; Lian, Z.; Wei, B.; Li, Y.; Bondarchuk, O.; Zhang, N.; Yu, Z. P.; Araujo, A.; Amorim, I.; Wang, Z. C. et al. Strong electronic coupling between ultrafine iridium-ruthenium nanoclusters and conductive, acid-stable tellurium nanoparticle support for efficient and durable oxygen evolution in acidic and neutral media. *ACS Catal.* **2020**, *10*, 3571–3579.
[90] Chen, P. Z.; Xu, K.; Fang, Z. W.; Tong, Y.; Wu, J. C.; Lu, X. L.; Peng, X.; Ding, H.; Wu, C. Z.; Xie, Y. Metallic Co_4N porous nanowire arrays activated by surface oxidation as electrocatalysts for the oxygen evolution reaction. *Angew. Chem., Int. Ed.* **2015**, *54*, 14710–14714.
[91] Zhang, W. M.; Yao, X. Y.; Zhou, S. N.; Li, X. W.; Li, L.; Yu, Z.; Gu, L. ZIF-8/ZIF-67-derived Co-N_x-embedded 1d porous carbon nanofibers with graphitic carbon-encased Co nanoparticles as an efficient bifunctional electrocatalyst. *Small* **2018**, *14*, 1800423.
[92] Zhao, Z. L.; Wu, H. X.; He, H. L.; Xu, X. L.; Jin, Y. D. A high-performance binary Ni-Co hydroxide-based water oxidation electrode with three-dimensional coaxial nanotube array structure. *Adv. Funct. Mater.* **2014**, *24*, 4698–4705.
[93] Shi, Q. R.; Zhu, C. Z.; Du, D.; Wang, J.; Xia, H. B.; Engelhard, M. H.; Feng, S.; Lin, Y. H. Ultrathin dendritic IrTe nanotubes for an efficient oxygen evolution reaction in a wide pH range. *J. Mater. Chem. A* **2018**, *6*, 8855–8859.
[94] Li, L. G.; Wang, P. T.; Cheng, Z. F.; Shao, Q.; Huang, X. Q. One-dimensional iridium-based nanowires for efficient water electrooxidation and beyond. *Nano Res.* **2022**, *15*, 1087–1093.
[95] Liu, M.; Liu, S. L.; Mao, Q. Q.; Yin, S. L.; Wang, Z. Q.; Xu, Y.;

Li, X. N. A.; Wang, L.; Wang, H. J. Ultrafine ruthenium-iridium-tellurium nanotubes for boosting overall water splitting in acidic media. *J. Mater. Chem. A* **2022**, *10*, 2021–2026.

[96] Wang, J.; Han, L. L.; Huang, B. L.; Shao, Q.; Xin, H. L.; Huang, X. Q. Amorphization activated ruthenium-tellurium nanorods for efficient water splitting. *Nat. Commun.* **2019**, *10*, 5692.

[97] Tang, B.; Yang, X. D.; Kang, Z. H.; Feng, L. G. Crystallized $RuTe_2$ as unexpected bifunctional catalyst for overall water splitting. *Appl. Catal. B* **2020**, *278*, 119281.

[98] Zhu, Y. P.; Guo, C. X.; Zheng, Y.; Qiao, S. Z. Surface and interface engineering of noble-metal-free electrocatalysts for efficient energy conversion processes. *Acc. Chem. Res.* **2017**, *50*, 915–923.

[99] Wang, H. P.; Zhu, S.; Deng, J. W.; Zhang, W. C.; Feng, Y. Z.; Ma, J. M. Transition metal carbides in electrocatalytic oxygen evolution reaction. *Chin. Chem. Lett.* **2021**, *32*, 291–298.

[100] Cui, X. J.; Ren, P. J.; Deng, D. H.; Deng, J.; Bao, X. H. Single layer graphene encapsulating non-precious metals as high-performance electrocatalysts for water oxidation. *Energy Environ. Sci.* **2016**, *9*, 123–129.

[101] Wang, X. X.; Li, L.; Xu, L. G.; Wang, Z.; Wu, Z. Y.; Liu, Z. L.; Yangs, P. An efficient and stable MnCo@NiS catalyst for oxygen evolution reaction constructed by a step-by-step electrodeposition way. *J. Power Sources* **2021**, *489*, 229525.

[102] Zhang, L. Z.; Chen, C.; Zhou, J. D.; Yang, G. L.; Wang, J. M.; Liu, D.; Chen, Z. Q.; Lei, W. W. Solid phase exfoliation for producing dispersible transition metal dichalcogenides nanosheets. *Adv. Funct. Mater.* **2020**, *30*, 2004139.

[103] Zhang, Y. Y.; Xiao, G.; Wang, H.; Lin, Y. X. Effect of O, Se and Te doping on the electronic band structure and optical properties of single layer MoS_2. *J. Synth. Cryst.* **2017**, *46*, 1665–1671.

[104] Wang, D.; Chang, Y. X.; Li, Y. R.; Zhang, S. L.; Xu, S. L. Well-dispersed $NiCoS_2$ nanoparticles/rGO composite with a large specific surface area as an oxygen evolution reaction electrocatalyst. *Rare Met.* **2021**, *40*, 3156–3165.

[105] Gao, G. P.; Jiao, Y.; Ma, F. X.; Jiao, Y. L.; Waclawik, E.; Du, A. J. Charge mediated semiconducting-to-metallic phase transition in molybdenum disulfide monolayer and hydrogen evolution reaction in new 1T' phase. *J. Phys. Chem. C* **2015**, *119*, 13124–13128.

[106] Ambrosi, A.; Sofer, Z.; Pumera, M. 2H→1T phase transition and hydrogen evolution activity of MoS_2, $MoSe_2$, WS_2 and WSe_2 strongly depends on the MX_2 composition. *Chem. Commun.* **2015**, *51*, 8450–8453.

[107] Wang, D. Z.; Zhang, X. Y.; Bao, S. Y.; Zhang, Z. T.; Fei, H.; Wu, Z. Z. Phase engineering of a multiphasic 1T/2H MoS_2 catalyst for highly efficient hydrogen evolution. *J. Mater. Chem. A* **2017**, *5*, 2681–2688.

[108] Wang, S.; Zhang, D.; Li, B.; Zhang, C.; Du, Z. G.; Yin, H. M.; Bi, X. F.; Yang, S. B. Ultrastable in-plane 1T-2H MoS_2 heterostructures for enhanced hydrogen evolution reaction. *Adv. Energy Mater.* **2018**, *8*, 1801345.

[109] Friebel, D.; Louie, M. W.; Bajdich, M.; Sanwald, K. E.; Cai, Y.; Wise, A. M.; Cheng, M. J.; Sokaras, D.; Weng, T. C.; Alonso-Mori, R. et al. Identification of highly active Fe sites in (Ni, Fe)OOH for electrocatalytic water splitting. *J. Am. Chem. Soc.* **2015**, *137*, 1305–1313.

[110] Wang, H. Y.; Hung, S. F.; Chen, H. Y.; Chan, T. S.; Chen, H. M.; Liu, B. *In operando* identification of geometrical-site-dependent water oxidation activity of spinel Co_3O_4. *J. Am. Chem. Soc.* **2016**, 138, 36–39.

[111] Lee, S.; Banjac, K.; Lingenfelder, M.; Hu, X. L. Oxygen isotope labeling experiments reveal different reaction sites for the oxygen evolution reaction on nickel and nickel iron oxides. *Angew. Chem., Int. Ed.* **2019**, *58*, 10295–10299.

[112] Wang, Z. Y.; Jiang, S. D.; Duan, C. Q.; Wang, D.; Luo, S. H.; Liu, Y. G. *In situ* synthesis of Co_3O_4 nanoparticles confined in 3D nitrogen-doped porous carbon as an efficient bifunctional oxygen electrocatalyst. *Rare Met.* **2020**, *39*, 1383–1394.

[113] Gao, Q.; Huang, C. Q.; Ju, Y. M.; Gao, M. R.; Liu, J. W.; An, D.; Cui, C. H.; Zheng, Y. R.; Li, W. X.; Yu, S. H. Phase-selective syntheses of cobalt telluride nanofleeces for efficient oxygen evolution catalysts. *Angew. Chem., Int. Ed.* **2017**, *56*, 7769–7773.

[114] Majhi, K. C.; Karfa, P.; Madhuri, R. Bimetallic transition metal chalcogenide nanowire array: An effective catalyst for overall water splitting. *Electrochim. Acta* **2019**, *318*, 901–912.

[115] Ji, L. L.; Wang, J. Y.; Teng, X.; Meyer, T. J.; Chen, Z. F. CoP nanoframes as bifunctional electrocatalysts for efficient overall water splitting. *ACS Catal.* **2020**, *10*, 412–419.

[116] Chen, Z. L.; Chen, M.; Yan, X. X.; Jia, H. X.; Fei, B.; Ha, Y.; Qing, H. L.; Yang, H. Y.; Liu, M.; Wu, R. B. Vacancy occupation-driven polymorphic transformation in cobalt ditelluride for boosted oxygen evolution reaction. *ACS Nano* **2020**, *14*, 6968–6979.

[117] He, B.; Wang, X. C.; Xia, L. X.; Guo, Y. Q.; Tang, Y. W.; Zhao, Y.; Hao, Q. L.; Yu, T.; Liu, H. K.; Su, Z. Metal-organic framework-derived Fe-doped $Co_{1.11}Te_2$ embedded in nitrogen-doped carbon nanotube for water splitting. *ChemSusChem* **2020**, *13*, 5239–5247.

[118] Bhat, K. S.; Barshilia, H. C.; Nagaraja, H. S. Porous nickel telluride nanostructures as bifunctional electrocatalyst towards hydrogen and oxygen evolution reaction. *Int. J. Hydrogen Energy* **2017**, *42*, 24645–24655.

[119] Wang, Q.; Zhu, J. Y.; Wang, H. H.; Yu, S. C.; Wu, X. H. Anchoring NiTe domains with unusual composition on $Pb_{0.95}Ni_{0.05}Te$ nanorod as superior lithium-ion battery anodes and oxygen evolution catalysts. *Mater. Today Energy* **2019**, *11*, 199–210.

[120] De Silva, U.; Masud, J.; Zhang, N.; Hong, Y.; Liyanage, W. P. R.; Zaeem, M. A.; Nath, M. Nickel telluride as a bifunctional electrocatalyst for efficient water splitting in alkaline medium. *J. Mater. Chem. A* **2018**, *6*, 7608–7622.

[121] Sadaqat, M.; Manzoor, S.; Nisar, L.; Hassan, A.; Tyagi, D.; Shah, J. H.; Ashiq, M. N.; Joya, K. S.; Alshahrani, T.; Najam-ul-Haq, M. Iron doped nickel ditelluride hierarchical nanoflakes arrays directly grown on nickel foam as robust electrodes for oxygen evolution reaction. *Electrochim. Acta* **2021**, *371*, 137830.

[122] Pan, U. N.; Paudel, D. R.; Das, A. K.; Singh, T. I.; Kim, N. H.; Lee, J. H. Ni-nanoclusters hybridized 1T-Mn-VTe_2 mesoporous nanosheets for ultra-low potential water splitting. *Appl. Catal. B* **2022**, *301*, 120780.

[123] Zhang, W. Q.; Wang, J.; Zhao, L. L.; Wang, J. R.; Zhao, M. W. Transition-metal monochalcogenide nanowires: Highly efficient bi-functional catalysts for the oxygen evolution/reduction reactions. *Nanoscale* **2020**, *12*, 12883–12890.

[124] Kou, Z. K.; Yu, Y.; Liu, X. M.; Gao, X. R.; Zheng, L. R.; Zou, H. Y.; Pang, Y. J.; Wang, Z. Y.; Pan, Z. H.; He, J. Q. et al. Potential-dependent phase transition and Mo-enriched surface reconstruction of γ-CoOOH in a heterostructured Co-Mo_2C precatalyst enable water oxidation. *ACS Catal.* **2020**, *10*, 4411–4419.

[125] Qin, J. F.; Yang, M.; Chen, T. S.; Dong, B.; Hou, S.; Ma, X.; Zhou, Y. N.; Yang, X. L.; Nan, J.; Chai, Y. M. Ternary metal sulfides MoCoNiS derived from metal organic frameworks for efficient oxygen evolution. *Int. J. Hydrogen Energy* **2020**, *45*, 2745–2753.

[126] He, R. Z.; Li, M.; Qiao, W.; Feng, L. G. Fe doped Mo/Te nanorods with improved stability for oxygen evolution reaction. *Chem. Eng. J.* **2021**, *423*, 130168.

[127] Inamdar, A. I.; Chavan, H. S.; Hou, B.; Lee, C. H.; Lee, S. U.; Cha, S.; Kim, H.; Im, H. A robust nonprecious CuFe composite as a highly efficient bifunctional catalyst for overall electrochemical water splitting. *Small* **2020**, *16*, 1905884.

[128] Zu, M. Y.; Wang, C. W.; Zhang, L.; Zheng, L. R.; Yang, H. G. Reconstructing bimetallic carbide Mo_6Ni_6C for carbon interconnected MoNi alloys to boost oxygen evolution electrocatalysis. *Mater. Horiz.* **2019**, *6*, 115–121.

[129] He, Q.; Li, S. L.; Huang, S. W.; Xiao, L. Q.; Hou, L. X. Construction of uniform Co-Sn-X (X = S, Se, Te) nanocages with enhanced photovoltaic and oxygen evolution properties via anion exchange reaction. *Nanoscale* **2018**, *10*, 22012–22024.

[130] Majhi, K. C.; Karfa, P.; De, S.; Madhuri, R. Hydrothermal synthesis of zinc cobalt telluride nanorod towards oxygen evolution reaction

(OER). In *International Conference on Advances in Materials and Manufacturing Applications (IConAMMA)*, IOP Publishing Ltd., Bengaluru, India, 2018.
[131] Qian, G. F.; Mo, Y. S.; Yu, C.; Zhang, H.; Yu, T. Q.; Luo, L.; Yin, S. B. Free-standing bimetallic $CoNiTe_2$ nanosheets as efficient catalysts with high stability at large current density for oxygen evolution reaction. *Renew. Energy* **2020**, *162*, 2190–2196.
[132] Su, M. Y.; Li, X. Y.; Zhang, J. T. Telluride semiconductor nanocrystals: Progress on their liquid-phase synthesis and applications. *Rare Met.* **2022**, *41*, 2527–2551.
[133] Na, J. H.; Hoyer, A.; Schoop, L.; Weber, D.; Lotsch, B. V.; Burghard, M.; Kern, K. Tuning the magnetoresistance of ultrathin WTe_2 sheets by electrostatic gating. *Nanoscale* **2016**, *8*, 18703–18709.
[134] Yoo, Y.; DeGregorio, Z. P.; Su, Y.; Koester, S. J.; Johns, J. E. In-Plane 2H-1T′ $MoTe_2$ homojunctions synthesized by flux-controlled phase engineering. *Adv. Mater.* **2017**, *29*, 1605461.
[135] Hu, L. Y.; Zeng, X.; Wei, X. Q.; Wang, H. J.; Wu, Y.; Gu, W. L.; Shi, L.; Zhu, C. Z. Interface engineering for enhancing electrocatalytic oxygen evolution of NiFe LDH/NiTe heterostructures. *Appl. Catal. B* **2020**, *273*, 119014.
[136] Sun, Y. F.; Wang, Y. X.; Sun, D.; Carvalho, B. R.; Read, C. G.; Lee, C. H.; Lin, Z.; Fujisawa, K.; Robinson, J. A.; Crespi, V. H. et al. Low-temperature solution synthesis of few-layer 1T′-$MoTe_2$ nanostructures exhibiting lattice compression. *Angew. Chem., Int. Ed.* **2016**, *55*, 2830–2834.
[137] Ma, R.; Cui, X.; Wang, Y. L.; Xiao, Z. Y.; Luo, R.; Gao, L. K.; Wei, Z. N.; Yang, Y. K. Pyrolysis-free synthesis of single-atom cobalt catalysts for efficient oxygen reduction. *J. Mater. Chem. A* **2022**, *10*, 5918–5924.
[138] Cui, X.; Lei, S.; Wang, A. C.; Gao, L. K.; Zhang, Q.; Yang, Y. K.; Lin, Z. Q. Emerging covalent organic frameworks tailored materials for electrocatalysis. *Nano Energy* **2020**, *70*, 104525.
[139] Cui, X.; Gao, L. K.; Lei, S.; Liang, S.; Zhang, J. W.; Sewell, C. D.; Xue, W. D.; Liu, Q.; Lin, Z. Q.; Yang, Y. K. Simultaneously crafting single-atomic Fe sites and graphitic layer-wrapped Fe_3C nanoparticles encapsulated within mesoporous carbon tubes for oxygen reduction. *Adv. Funct. Mater.* **2021**, *31*, 2009197.
[140] Liu, K.; Fu, J. W.; Lin, Y. Y.; Luo, T.; Ni, G. H.; Li, H. M.; Lin, Z.; Liu, M. Insights into the activity of single-atom Fe-N-C catalysts for oxygen reduction reaction. *Nat. Commun.* **2022**, *13*, 2075.

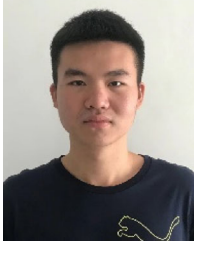

Feng Gao received his B.S. degree from Sun Yat-Sen University. He is currently pursuing his Ph.D. degree under the supervision of Prof. Mengye Wang in Sun Yat-Sen University. His current research focuses on electrocatalytic water splitting.

Dr. Mengye Wang is an Associate Professor in the School of Materials at Sun Yat-Sen University. She received her PhD degree in Physical Chemistry from Xiamen University in 2015. She is the editorial board member for nine journals, including *Nano Research Energy*, *Nano Research*, *Materials Horizons*, *Journal of Materials Chemistry A*, *Materials Advances*, *Rare Metals*, *Journal of Synthetic Crystals*, *Journal of Physics D: Applied Physics*, and *Cleaner Materials*. Her research interests include upcycling solid wastes and advanced materials for environmental and energy related applications.